Quantum Simulation

Bachelor's Degree Thesis
Submitted to the Faculty at the
Escola Tècnica Superior
d'Enginyeria de Telecomunicació de Barcelona
of the Universitat Politècnica de Catalunya
by

Albert López Escudero

In partial fulfillment
of the requirements for the
DEGREE IN ELECTRONICS ENGINEERING

Advisor: Vincenzo de Maio & Ivona Bandric
Reviewer: Javier Rodrigez Fonollosa

Barcelona, January 2025

ETSETB – Degree in Electronics Engineering

Resum

Cada exemplar del Treball de Fi de Grau (TFG) ha de contenir un Resum, que és un breu extracte del TFG. En termes d'estil, el Resum hauria de ser una versió reduïda del projecte: una introducció concisa, un compendi dels resultats i les principals conclusions o arguments presentats en el projecte. El Resum no ha de superar les 150 paraules i cal que estigui traduït al català, castellà i anglès.

Resumen

Cada ejemplar del Trabajo de Fin de Grado (TFG) debe incluir un Resumenque es un breve extracto del TFG. En cuanto al estilo, el Resumen debería ser una versión reducida del proyecto: una introducción breve, un resumen de los resultados principales y las conclusiones o argumentos principales presentados en el proyecto. El Resumen no debe exceder las 150 palabras y debe estar traducido al catalán, castellano e inglés.

Summary

Each copy of the Bachelor's Thesis (TFG) must include a Summary, which is a concise abstract of the TFG. In terms of style, the Summary should be a condensed version of the project: a brief introduction, a summary of the main results, and the conclusions or key arguments presented in the project. The Summary should not exceed 150 words and must be translated to catalan, spanish and english.

A Dedication page may be included in your thesis just before the Acknowledgments page, but it is not a requirement.

Acknowledgements

It is appropriate, but not mandatory, to declare the extent to which assistance has been given by members of the staff, fellow students, technicians or others in the collection of materials and data, the design and construction of apparatus, the performance of experiments, the analysis of data, and the preparation of the thesis (including editorial help). In addition, it is appropriate to recognize the supervision and advice given by your advisor.

Revision history and approval record

Revision	Date	Author(s)	Description
1.0	dd/mm/yyyy	AME	Document creation
1.1	dd/mm/yyyy	AME, JPV	Error correction
2.0	dd/mm/yyyy	AME, MLO	Revised after review
4.0	dd/mm/yyyy	AME	Final version

DOCUMENT DISTRIBUTION LIST

Role	Surname(s) and Name
[Student]	
[Project Supervisor 1]	
[Project Supervisor 2 (if applicable)]	

Written by:		Reviewed and approved by:	
Date	dd/mm/yyyy	Date	dd/mm/yyyy
Name	Xxxxxxx Yyyyyyy	Name	Xxxxxxx Yyyyyyy
Position	Project Author	Position	Project Supervisor

Contents

List of Figures

List of Tables

Abbreviations

Adagrad	Adaptive Gradient Algorithm
Adam	Adaptive Moment Estimation
ADAPT-VQE	Adaptive Variational Quantum Eigensolver
AQS	Analog Quantum Simulation
CCSD	Coupled Cluster with Singles and Doubles
CPU	Central Processing Unit
DQS	Digital Quantum Simulation
ETSETB	Escola Tècnica Superior d'Enginyeria de Telecomunicació de Barcelona
EU	European Union
FCI	Full Configuration Interaction
GD	Gradient Descent
GEF	Grau en Enginyeria Física
GPU	Graphics Processing Unit
GREELEC	Grau en Enginyeria Electrònica de Telecomunicació
HF	Hartree-Fock
MPS	Matrix Product States
NISQ	Noisy Intermediate-Scale Quantum
NMomentum	Nesterov Momentum
PEPS	Projected Entangled Pair States
QNG	Quantum Natural Gradient
RMSProp	Root Mean Square Propagation
UCCSD	Unitary Coupled Cluster with Singles and Doubles
VQE	Variational Quantum Eigensolver

CHAPTER 1

Introduction

In recent years, computing has undergone significant evolution, reaching a point where improving the hardware of traditional devices presents considerable challenges. This has driven research in quantum computing, a technology that promises to revolutionize the field by enabling much more efficient calculations and superior processing capabilities. In applications such as molecular simulation, quantum computing has proven to be remarkably more efficient than classical computing, justifying investment in its development.

However, one of the main obstacles of quantum computing is the high cost associated with its devices. To run programs on a quantum computer, it must operate at extremely low temperatures, close to 0.1 Kelvin, which significantly increases the cost and technical complexity. Therefore, methods are being investigated to improve and optimize these devices, making them more accessible and viable for broader use.

Currently, one of the most practical ways to harness quantum computing's potential is through **quantum simulation**. Quantum simulation allows us to study complex quantum systems using either quantum simulators or classical computers. By emulating the behavior of quantum systems, we can explore quantum algorithms and applications effectively without necessarily requiring a fully functional quantum computer.

The main objective of this project is to develop a quantum simulator capable of efficiently modeling molecules using advanced quantum algorithms, with a specific focus on implementing the Variational Quantum Eigensolver (VQE) algorithm. This algorithm combines quantum circuits for state preparation and classical optimizers that adjust parameters to minimize the system's energy. Additionally, the project introduces innovations in the design of adaptive quantum circuits, the integration of simultaneous optimizations of nuclear and electronic coordinates, all within a modular and extensible project structure that allows for easy and effective adaptation of the simulation.

1.1 Work goals

The primary goal of this project is to contribute a novel methodology to the field of molecular simulations by:

- Optimize the quantum simulation framework to minimize computational overhead while maintaining accuracy in modeling molecular systems, focusing on enhancing the Variational Quantum Eigensolver (VQE) efficiency.
- Develop an adaptive quantum ansatz capable of dynamically selecting and integrating operators with the highest impact on performance, ensuring rapid convergence and reduced computational cost.
- Integrate advanced hybrid optimization cycles that streamline both electronic state and nuclear geometry refinements, with an emphasis on computational speed and scalability.
- Design a high-performance, modular architecture tailored for extensibility, facilitating the efficient inclusion of cutting-edge algorithms, ansatz designs, and optimization strategies.

1.2 Requirements and specifications

To achieve these objectives, the following requirements and specifications have been established:

- **Dynamic Ansatz Construction**: Integrate an adaptive ansatz mechanism that employs energy gradient calculations to iteratively select and include the most impactful operators, reducing the complexity of the quantum circuits without compromising accuracy.
- **Advanced Hybrid Optimization**: Develop a unified optimization cycle combining variational parameter updates and nuclear geometry refinements, supported by precise gradient-based techniques. Ensure the use of optimizers for rapid convergence and enhanced stability.
- **Scalable Hamiltonian Management**: Implement a modular Hamiltonian construction process that accommodates different molecular geometries and basis sets with efficient computation of molecular properties.
- **Efficient Gradient Computation**: Optimize gradient calculations for both quantum and nuclear coordinates using automatic differentiation, enabling simultaneous updates and faster convergence.
- **Performance Monitoring and Visualization**: Develop tools for tracking energy convergence, execution time, and molecular geometry evolution. Include detailed visualizations (e.g., energy evolution plots, 3D geometries) to ensure transparency and allow performance analysis.

- **Extensibility and Modularity**: Ensure a modular project structure that facilitates the inclusion of new ansatz types, optimizers, and molecular systems with minimal adjustments. Employ a structured directory for clear separation of functionality and scalability.
- **Parallel Execution Capability**: Leverage multiprocessing capabilities to evaluate multiple optimizers and configurations in parallel, enabling comprehensive performance analysis across various configurations.

1.3 Methods and procedures

In our project, we have implemented a series of advanced methodologies that integrate quantum and classical techniques with specific innovations to address molecular optimization problems and energy calculations efficiently. We have combined quantum computing, which enables the evaluation of fundamental system properties such as energy and quantum states, with classical algorithms that optimize the parameters required to represent these states effectively. This hybrid approach, inspired by the ideas of Richard Feynman, has been validated in works like that of Arute et al. (2019), who achieved quantum supremacy using digital circuits to solve problems inaccessible to classical computers. Within this framework, we used the Variational Quantum Eigensolver (VQE) algorithm as the core of our simulation. This algorithm combines parameterized circuits, known as ansatz, with classical optimization to minimize the expected value of the molecular Hamiltonian, which describes the total energy of the system. Introduced by Peruzzo et al. in 2014, VQE has proven particularly effective for noisy intermediate-scale quantum (NISQ) devices.

Additionally, we have implemented an adaptive ansatz that enhances efficiency by dynamically constructing the quantum circuit. This ansatz iteratively selects relevant operators based on energy gradients, an approach inspired by the ADAPT-VQE algorithm by Grimsley et al. (2019), ensuring faster and more accurate convergence to the ground state. Since scalable quantum hardware is not available, we used classical simulators such as PennyLane's default.qubit to emulate digital quantum circuits. This has allowed us to design and evaluate algorithms robustly in classical environments while maintaining the ability to test innovative approaches.

Among the main innovations implemented, we developed a dynamic adaptive ansatz that incorporates only the quantum operators with the greatest impact on energy, calculated through gradients using automatic differentiation. This not only optimizes computational efficiency but also reduces the complexity of the model. We also implemented a hybrid optimization cycle that simultaneously adjusts the ansatz parameters and nuclear positions, accurately capturing the interaction between electrons and molecular geometry. The modular structure of the code has been key to enabling the incorporation of new functionalities and the comparison of different optimization strategies without affecting other components of the system. Finally, we designed the system to support multiple types of ansatz and optimizers, facilitating an exhaustive comparative analysis and ensuring the scalability of the project for future extensions in quantum chemistry and molecular simulations.

1.4 Work plan

During the development of the project, the initial plan was largely followed. However, several complications arose that extended some deadlines, requiring adjustments to the overall timeline to achieve the established objectives.

The main setback was related to the integration of the JAX interface. From the outset, we were confident that using JAX would significantly improve the performance of the simulations. However, upon completing the initial integration, we were surprised to find that the performance not only failed to improve but actually worsened. This unexpected result led us to conduct more checks than initially planned, aiming to verify the accuracy of the results and identify the root cause of this behavior.

This situation caused delays in the second phase of the project, which, in turn, required a reduction in the time allocated to the third phase to meet the deadlines. Despite this, we decided not to compromise on the quality of the project. As a result, the overall development time had to be extended, increasing the daily hours dedicated to the project. This additional effort ensured that the initial objectives were achieved without compromising the proposed quality standards.

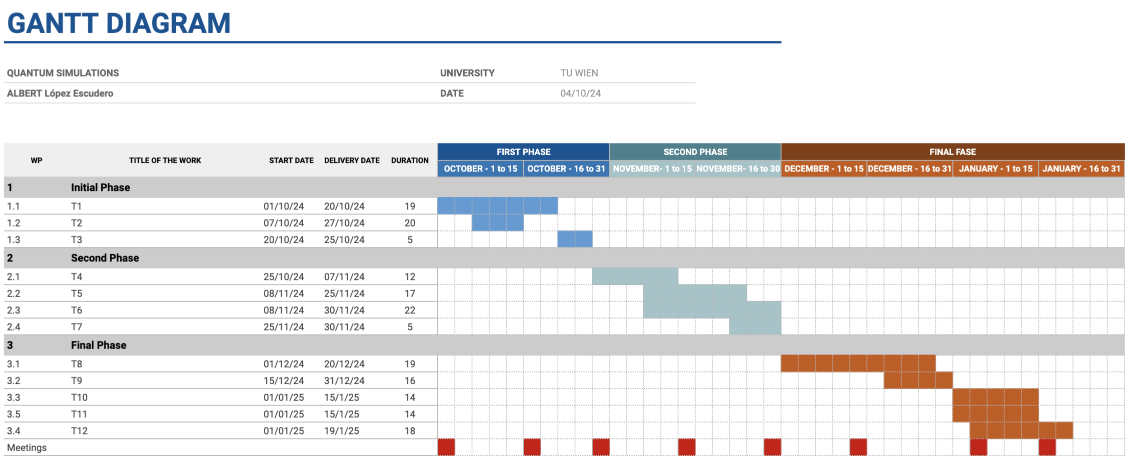

QUANTUM SIMULATIONS		UNIVERSITY	TU WIEN
ALBERT López Escudero		DATE	04/10/24

WP	TITLE OF THE WORK	START DATE	DELIVERY DATE	DURATION
1	Initial Phase			
1.1	T1	01/10/24	20/10/24	19
1.2	T2	07/10/24	27/10/24	20
1.3	T3	20/10/24	25/10/24	5
2	Second Phase			
2.1	T4	25/10/24	07/11/24	12
2.2	T5	08/11/24	25/11/24	17
2.3	T6	08/11/24	30/11/24	22
2.4	T7	25/11/24	30/11/24	5
3	Final Phase			
3.1	T8	01/12/24	20/12/24	19
3.2	T9	15/12/24	31/12/24	16
3.3	T10	01/01/25	15/1/25	14
3.5	T11	01/01/25	15/1/25	14
3.4	T12	01/01/25	19/1/25	18
Meetings				

Figure 1.1: *Gantt diagram showing the project timeline and the distribution of tasks over the development period.*

CHAPTER 2

State of the Art of the Technology Used or Applied in this Thesis

In this project, we focus on the operation of quantum simulators applied to molecular simulation, an area where quantum computing offers significant advantages. The main objective is to develop a program capable of simulating different molecules in a simple and efficient manner.

To this end, we will review the basic concepts of quantum mechanics that are essential to understand the fundamentals and potential of quantum computing, and explore the techniques of quantum simulation that allow us to harness quantum computing capabilities even with current technological limitations.

2.1 Quantum Simulation

Quantum simulation has emerged as an advanced and essential technique for studying complex quantum systems, especially those that are inaccessible or present great challenges for direct analysis using classical methods. Based on the proposal of Richard Feynman, who postulated that a computer built from quantum elements could overcome the limitations of classical computers in simulating quantum phenomena, quantum simulation has progressed significantly. It encompasses both digital and analog simulations and has expanded its applicability in various scientific areas.

There are mainly two approaches in quantum simulation: **Digital Quantum Simulation (DQS)** and **Analog Quantum Simulation (AQS)**. DQS employs the quantum circuit model, where systems are represented by qubits that evolve through quantum gates to reproduce the dynamics of the target system. This approach is universal, as it can, in principle, simulate any quantum system, although not always efficiently. On the other hand, AQS involves creating a quantum system that directly emulates the Hamiltonian of the system under study, allowing certain properties of the simulated system, such as time evolution, to be reproduced approximately. This method is particularly useful when a qualitative representation is required rather than high precision.

In addition to these approaches, there are algorithms inspired by quantum information theory that facilitate the classical simulation of quantum systems. Techniques such as **Matrix Product States (MPS)** and **Projected Entangled Pair States (PEPS)** allow representing particle systems on classical computers more efficiently than standard classical methods, optimizing the calculation of properties of complex quantum systems.

The applications of quantum simulation are broad and encompass multiple scientific fields. In condensed matter physics, it allows the study of models such as the Hubbard model and quantum phase transitions, fundamental for understanding phenomena like superconductivity. In quantum chemistry, it facilitates the calculation of molecular energies and complex chemical reactions. In high-energy physics and cosmology, it emulates particles in high-energy fields and cosmological phenomena. Furthermore, quantum simulation is instrumental in the analysis of open quantum systems and in the investigation of quantum chaos, allowing exploration of interactions with the environment and chaotic dynamics in the quantum realm.

However, quantum simulation faces significant challenges related to the precise control of the quantum simulator systems and the management of decoherence and errors, which can affect the accuracy of the results. The amount of required resources, such as the number of qubits and quantum gates, also depends on the size and complexity of the system to be simulated. It is estimated that quantum simulators require between 40 and 100 qubits to surpass the computational power of classical computers in specific problems. Despite these challenges, technological advances continue to improve the viability and efficiency of quantum simulation, promising to transform research in natural sciences and expand our understanding of quantum phenomena.

2.2 Key Concepts in Quantum Mechanics

It is essential to understand the difference between bits in classical computing and qubits in quantum computing to delve into this new technological paradigm.

In classical computing, the basic unit of information is the **bit**, which can take the value of 0 or 1. These bits are the foundation upon which conventional computers operate, processing information through combinations of these binary states.

In contrast, quantum computing uses the **qubit** or quantum bit as its basic unit. Unlike the classical bit, a qubit can exist in a superposition of states, meaning it can simultaneously represent the values 0 and 1 thanks to the principle of superposition in quantum mechanics. This property, along with phenomena such as quantum entanglement and interference, allows quantum computers to process information exponentially more efficiently for certain problems.

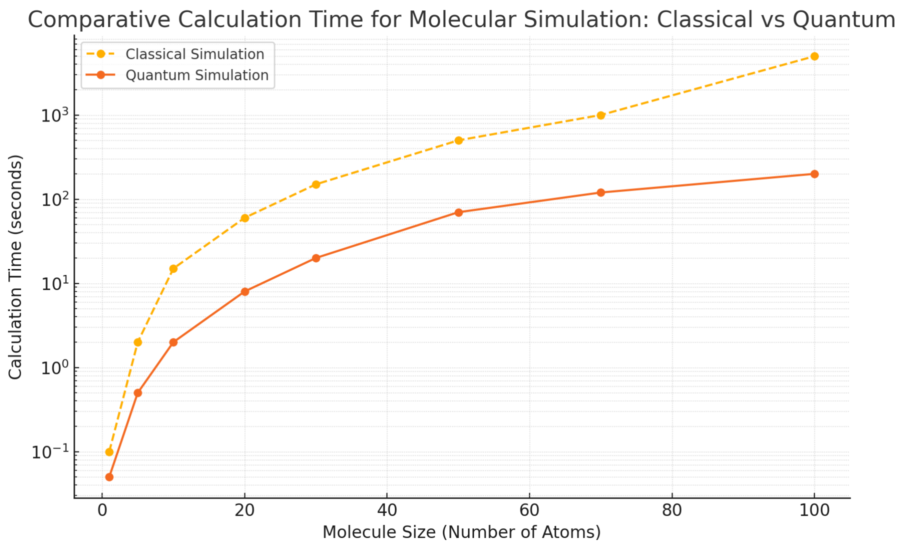

Figure 2.1: *Comparison of computation time for molecular simulations: classical vs quantum.*

Understanding how qubits operate and their differences from classical bits is essential to appreciate the revolutionary potential of quantum computing.

2.2.1 Qubit

The **qubit** is the basic unit of information in quantum computing. While the classical bit can only be in one of two states (0 or 1), a qubit can be in a superposition of both states simultaneously. This is due to the principle of quantum superposition, one of the fundamental characteristics of quantum mechanics.

Mathematically, a qubit is represented as a linear combination of the basis states $|0\rangle$ and $|1\rangle$:

$$|\psi\rangle = \alpha\,|0\rangle + \beta\,|1\rangle$$

where α and β are complex numbers that satisfy the normalization condition $|\alpha|^2+|\beta|^2 = 1$. These coefficients indicate the probability amplitudes of finding the qubit in the states $|0\rangle$ or $|1\rangle$ upon measurement.

In addition to superposition, qubits can exhibit **quantum entanglement**, a property that allows creating strong correlations between qubits that cannot be explained by classical physics. Entanglement is essential for the computational power of quantum computers, as it enables processing and storing an exponentially larger amount of information than classical systems.

For example, while a classical system of n bits can represent one of 2^n possible state combinations, a quantum system of n qubits can represent a superposition of all those combinations simultaneously. This capability is what allows quantum computers to tackle complex problems more efficiently.

However, manipulating and maintaining qubits is a significant technical challenge. Qubits are extremely sensitive and can be affected by interactions with the environment, leading to **quantum decoherence**. To minimize this effect and preserve quantum properties, it is necessary to keep systems in controlled conditions, such as very low temperatures, close to absolute zero.

2.2.2 Quantum Superposition

Quantum superposition allows a quantum system to exist in multiple states simultaneously until a measurement is performed. This characteristic is key to the functioning of quantum computers, as it enables processing a large amount of information in parallel.

In quantum systems, superposition is combined with **quantum interference**, where the probability amplitudes of states can reinforce or cancel each other out. This phenomenon is exploited in quantum algorithms to increase the probability of obtaining the correct result. For example, in Grover's algorithm, constructive interference amplifies the probability of the desired state, significantly improving the efficiency of searching for elements in an unsorted database.

Superposition is especially useful in simulating complex molecular systems. Quantum computers can naturally model the superpositions of electronic states in molecules, which is crucial for studying chemical reactions and molecular properties that are difficult to address with classical methods due to the exponential growth of computational resources required.

2.2.3 Quantum Decoherence

Quantum decoherence is one of the main challenges in quantum computing. It refers to the loss of a system's quantum properties, such as superposition and entanglement, due to unwanted interactions with the environment. This loss causes the quantum system to transition toward classical behavior, affecting the accuracy and reliability of quantum calculations.

Qubits are extremely sensitive to external disturbances, such as electromagnetic fluctuations, vibrations, and temperature changes. These interactions can cause quantum states to mix with those of the environment, leading to a loss of coherence that is irreversible and degrades the stored quantum information.

To mitigate the effects of decoherence, various strategies are implemented:

- **System Isolation**: Designing physical systems that minimize unwanted interactions with the environment, using materials and techniques that protect qubits from external disturbances.

- **Quantum Error Correction**: Implementing error correction codes that allow detecting and correcting errors without directly measuring the qubit's state, thereby preserving quantum information.
- **Dynamic Control**: Applying techniques such as pulse refocusing and dynamic pulse sequences that actively compensate for disturbances and extend the coherence time of qubits.

Controlling and mitigating decoherence are essential for the advancement of quantum computing and its application in areas like molecular simulation, where the precision of calculations is fundamental.

2.3 The Hamiltonian in Quantum Mechanics

The Hamiltonian is a fundamental concept originating from classical mechanics, introduced by William Rowan Hamilton in 1833. Hamiltonian mechanics is a reformulation of classical mechanics that provides powerful tools for studying the dynamics of systems. The Hamiltonian function represents the total energy of the system, expressed in terms of generalized coordinates and momenta, and is given by the sum of the kinetic and potential energies.

In quantum mechanics, the **Hamiltonian operator** plays a central role in describing the energy and time evolution of quantum systems. It represents the total energy of the system, including both kinetic and potential energies, and is essential for formulating the Schrödinger equation.

2.3.1 Mathematical Definition

The Hamiltonian operator, commonly denoted as $\hat{H}$, is a self-adjoint operator acting on the Hilbert space associated with the quantum system. For a single particle in one dimension, the Hamiltonian is expressed as:

$$\hat{H} = \hat{T} + \hat{V}$$

where:

- $\hat{T}$ is the kinetic energy operator.
- $\hat{V}$ is the potential energy operator.

In terms of the position $\hat{x}$ and momentum $\hat{p}$ operators, these are defined as:

$$\hat{T} = \frac{\hat{p}^2}{2m} = -\frac{\hbar^2}{2m}\frac{d^2}{dx^2}$$

$$\hat{V} = V(\hat{x})$$

Here, m is the mass of the particle, $\hbar$ is the reduced Planck constant, and $V(\hat{x})$ is the potential energy function depending on position.

2.3.2 Role in the Schrödinger Equation

The Hamiltonian is central to the Schrödinger equation, which describes how the quantum state of a system evolves over time. The time-dependent Schrödinger equation is expressed as:

$$i\hbar\frac{\partial}{\partial t}|\psi(t)\rangle = \hat{H}|\psi(t)\rangle$$

where $|\psi(t)\rangle$ is the state vector of the system at time t. For time-independent systems, the Schrödinger equation reduces to the eigenvalue equation:

$$\hat{H}|\psi\rangle = E|\psi\rangle$$

Here, E represents the eigenvalues of the Hamiltonian, corresponding to the allowed energy levels of the system, and $|\psi\rangle$ are the associated eigenstates.

2.3.3 Hamiltonian in Multi-Particle Systems

For systems with multiple particles, the Hamiltonian includes additional terms representing interactions between particles. For example, for a system of two particles, the Hamiltonian is expressed as:

$$\hat{H} = \hat{T}_1 + \hat{T}_2 + \hat{V}_1 + \hat{V}_2 + \hat{V}_{12}$$

where:

- $\hat{T}_1$ and $\hat{T}_2$ are the kinetic energy operators of particles 1 and 2, respectively.
- $\hat{V}_1$ and $\hat{V}_2$ are the individual potential energy operators.
- $\hat{V}_{12}$ represents the potential interaction between the two particles.

2.3.4 Importance in Quantum Simulations

In quantum simulations, especially in algorithms like the Variational Quantum Eigensolver (VQE), the Hamiltonian is decomposed into a sum of simpler terms, often expressed in terms of Pauli operators. This decomposition facilitates implementation on quantum circuits and allows estimating the system's energy through measurements on qubits.

Understanding the structure and properties of the Hamiltonian is essential for modeling and simulating quantum systems, as it determines the possible energies and dynamics of the system under study.

2.4 VQE: Variational Quantum Eigensolver

Among the hybrid quantum-classical algorithms developed to address quantum simulation challenges, the *Variational Quantum Eigensolver (VQE)* has gained particular relevance. This method seeks to approximate the ground-state energy of a target Hamiltonian, such as the electronic Hamiltonian of a molecule, by efficiently combining quantum state preparation with classical optimization techniques.

2.4.1 Fundamental Principles and Stages of the Algorithm

VQE is founded on the **variational principle** of quantum mechanics, which states that the expectation value of the energy $E(\vec{\theta})$ for any normalized trial state $|\psi(\vec{\theta})\rangle$ is always an upper bound to the true ground-state energy E_0:

$$E(\vec{\theta}) = \langle\psi(\vec{\theta})|\,\hat{H}\,|\psi(\vec{\theta})\rangle \quad \geq \; E_0.$$

Because $E(\vec{\theta})$ depends on a set of parameters $\vec{\theta}$, the VQE algorithm iteratively updates these parameters to minimize $E(\vec{\theta})$. Once no further reduction in $E(\vec{\theta})$ is possible, the algorithm identifies the lowest value reached as an approximation of E_0.

In practice, VQE proceeds in a loop that integrates quantum and classical resources:

1. **Quantum State Preparation:** A parameterized quantum circuit, commonly termed an *ansatz*, is constructed with a set of adjustable parameters $\vec{\theta}$. This circuit leverages unitary gates (e.g., single-qubit rotations, entangling gates) to create a trial wavefunction:
$$|\psi(\vec{\theta})\rangle\,.$$

2. **Measurement of the Expected Energy:** The Hamiltonian $\hat{H}$ is decomposed into a sum of Pauli operators acting on the qubits. The expectation value $\langle\,\psi(\vec{\theta})\mid\hat{H}\mid\psi(\vec{\theta})\rangle$ is obtained by measuring the appropriate Pauli operators on the quantum device, typically requiring multiple circuit executions due to non-commuting terms.

3. **Classical Optimization:** The measured energy serves as a cost function, $E(\vec{\theta})$. A classical optimizer—such as *Gradient Descent* or *Adam*—then updates the parameters $\vec{\theta}$ to minimize this cost.

4. **Iteration and Convergence:** Steps 1–3 repeat until a convergence criterion is satisfied, for instance,
$$\left|E\big(\vec{\theta}_{k+1}\big) - E\big(\vec{\theta}_k\big)\right| \; < \; \delta,$$
where δ is a small threshold for energy differences. The final set $\vec{\theta}^*$ yields an approximate ground-state wavefunction and energy.

2.4.2 Advantages and Challenges

VQE has garnered extensive interest in fields like **quantum chemistry**, **materials science**, and even combinatorial optimization problems mapped to Hamiltonians. Its hybrid structure allows leveraging near-term quantum devices (with limited qubits and gate depths) while offloading resource-intensive tasks—such as parameter updates—to classical computers.

Despite its promise, VQE faces several practical hurdles:

- **Noise and Decoherence:** Real quantum devices suffer from errors that deteriorate the fidelity of prepared states and measurements, requiring error-mitigation strategies and noise-aware ansatz designs.
- **Barren Plateaus:** High-dimensional parameter spaces can contain large regions where gradients vanish, complicating the search for global minima.
- **Measurement Overhead:** Decomposing a Hamiltonian into many Pauli terms demands running multiple circuits, increasing sampling time and exposure to hardware noise.
- **Circuit Depth:** Accurate ansätze for complex systems may require deep circuits that quickly exceed the coherence times of current quantum processors.

2.4.3 Outlook in Quantum Simulation

Continuous improvements in both hardware (qubit quality, gate fidelity, and error-correction schemes) and software (advanced ansätze, better optimizers, error mitigation) keep driving VQE toward practical applications. Recent strategies such as *ADAPT-VQE*, which adaptively builds up an excitation operator set, and domain-specific ansätze integrated with error mitigation methods, further enhance VQE's accuracy for molecular systems.

As the number of qubits grows and quantum hardware matures, VQE is likely to become a central approach for tackling classically intractable problems in quantum chemistry, materials science, and beyond. Its flexible hybrid nature will continue to serve as a testbed for new optimization algorithms, ansatz designs, and measurement strategies, bridging current *Noisy Intermediate-Scale Quantum (NISQ)* devices with the longer-term ambition of fault-tolerant quantum computing.

2.5 Different Ansätze in Quantum Chemistry and Quantum Computing

In the context of variational quantum algorithms and quantum chemistry, an **ansatz** is a carefully chosen, often physically motivated, parametric form of the quantum state used to approximate the ground (or excited) state of a system described by a given Hamiltonian. The term *ansatz* originates from the German word "approach" or "initial guess," and it reflects the central idea that we propose a functional form (or circuit structure) for the wavefunction and then optimize the parameters in search of the lowest possible energy.

Within the framework of the Variational Quantum Eigensolver (VQE), the ansatz is implemented as a parameterized quantum circuit whose gates depend on a set of continuous variables $\vec{\theta}$. By measuring the expectation value of the Hamiltonian with respect to this trial state, one obtains an energy estimate $E(\vec{\theta})$ which is then iteratively minimized by a classical optimizer. The success of a VQE calculation hinges critically on the expressiveness and resource requirements (number of gates, circuit depth, etc.) of the chosen ansatz.

Several ansätze have been proposed to achieve a balance between accuracy and computational cost. Below, we summarize the most relevant approaches, highlighting their theoretical underpinnings and current usage in quantum simulation.

2.5.1 Hartree–Fock-based Ansätze (Classical Reference)

A historically important "classical" ansatz in quantum chemistry arises from the **Hartree–Fock (HF)** approximation. In this method, the total wavefunction is assumed to be a single Slater determinant constructed from one-particle orbitals. Although it captures the fundamental antisymmetry required by the Pauli exclusion principle, it neglects most of the electron correlation. Post-HF methods, such as Configuration Interaction (CI), Many-Body Perturbation Theory (MPn), and Coupled Cluster (CC), then build on this reference state by introducing additional terms that account for electron correlation.

- **Configuration Interaction (CI):** Expands the wavefunction in a basis of Slater determinants (excitations) beyond the HF reference. The Full CI approach is exact within the chosen basis but scales exponentially with system size. Truncated CI methods (CIS, CID, CISD, etc.) reduce the computational cost but still grow quickly with system size.

- **Coupled Cluster (CC):** Expresses the wavefunction via an exponential of excitation operators acting on the HF reference. Formally written as

  $$|\Psi_{\text{CC}}\rangle = e^{\hat{T}}|\Phi_{\text{HF}}\rangle,$$

  where $\hat{T}$ is the sum of cluster excitation operators (singles, doubles, triples, etc.). Although Coupled Cluster with Singles and Doubles (CCSD) is often accurate, further inclusion of triples and higher excitations can be required for strongly correlated systems.

In the context of classical methods, these **ansätze** serve as trial wavefunctions whose coefficients are optimized using high-performance classical algorithms. Their conceptual basis—constructing physically motivated trial states that capture crucial features of the system—carries over into quantum computing.

2.5.2 Unitary Coupled Cluster (UCC)

A key adaptation of the Coupled Cluster theory to quantum computing is the **Unitary Coupled Cluster (UCC)** ansatz. It modifies the standard CC exponential by making it explicitly unitary:

$$|\Psi_{\mathrm{UCC}}\rangle = e^{\hat{T}(\vec{\theta})-\hat{T}^\dagger(\vec{\theta})}\,|\Phi_{\mathrm{HF}}\rangle,$$

where $\hat{T}(\vec{\theta})$ is typically truncated to include only single and double excitations (UCCSD). This approach guarantees that the resulting operator is unitary, which is crucial for hardware implementations in quantum computing since all gates must be unitary transformations.

- **UCCSD (Singles and Doubles):** The most widespread version of UCC is truncated at single and double excitations:

  $$\hat{T}(\vec{\theta}) = \sum_{i,a} \theta_i^a \hat{a}_a^\dagger \hat{a}_i \; + \sum_{i,j,a,b} \theta_{i,j}^{a,b}\, \hat{a}_a^\dagger \hat{a}_b^\dagger \hat{a}_j \hat{a}_i \; + \cdots$$

  Here, i, j denote occupied orbitals and a, b virtual (unoccupied) orbitals. By exponentiating both $\hat{T}$ and $\hat{T}^\dagger$, the wavefunction stays normalized. However, the circuit depth can become large since implementing the exponential of a sum of non-commuting operators requires a trotterization or related approximation.

- **ADAPT-VQE and Variants:** To mitigate the high circuit cost, variants like *ADAPT-VQE* build up a UCC-type ansatz incrementally, selecting only those excitation operators that most significantly lower the energy at each step. This adaptive approach reduces the number of gates needed and often converges faster.

2.5.3 Problem-Inspired or Custom Ansätze

In some cases, **custom ansätze** are tailored to the specific physical or chemical system under investigation. For example, if certain symmetries (like particle number or spin) are known to be crucial for describing the ground state, one can design an ansatz that explicitly respects those symmetries. Such approaches can drastically reduce the parameter space and improve convergence, albeit with some additional effort in circuit design.

2.6 Optimizers

In quantum simulation algorithms such as the Variational Quantum Eigensolver (VQE), optimizers constitute a key element of the hybrid quantum-classical workflow. Their primary objective is to minimize the cost function

$$E(\vec{\theta}) = \langle \psi(\vec{\theta}) \mid \hat{H} \mid \psi(\vec{\theta}) \rangle,$$

where $\hat{H}$ represents the Hamiltonian of the system under study and $|\psi(\vec{\theta})\rangle$ is a parameterized quantum state, often referred to as the *ansatz*. After each quantum measurement, the optimizer updates the parameter vector $\vec{\theta}$ to guide the system toward the ground-state energy. This process is iterated until convergence, balancing the capabilities of quantum hardware with classical numerical techniques.

In the following subsections, we discuss the theoretical underpinnings and key features of several optimizers commonly employed in variational algorithms. While all these optimizers share the goal of efficiently navigating the parameter space, they differ in how they incorporate gradients, memory of past iterations, and adjustments of the learning rate.

2.6.1 Gradient Descent (GD)

Gradient Descent is one of the most fundamental methods for continuous optimization. At each iteration, it updates parameters by moving them in the direction opposite to the gradient of the cost function:

$$\vec{\theta}_{k+1} = \vec{\theta}_k - \eta \nabla_{\vec{\theta}} E(\vec{\theta}_k),$$

where η is the learning rate and $\nabla_{\vec{\theta}} E(\vec{\theta})$ denotes the gradient of the cost function with respect to the parameters. Despite its simplicity, Gradient Descent can converge slowly or get trapped in local minima when dealing with complex or high-dimensional landscapes, making it less efficient if used alone in large-scale molecular simulations.

2.6.2 Momentum Optimizer

The *Momentum* method extends standard Gradient Descent by incorporating a velocity term that accumulates a fraction of previous updates. This approach can mitigate oscillations and speed up convergence in regions with shallow gradients. The update rule is given by:

$$\begin{aligned}\vec{v}_{k+1} &= \gamma \vec{v}_k - \eta \nabla_{\vec{\theta}} E(\vec{\theta}_k),\\ \vec{\theta}_{k+1} &= \vec{\theta}_k + \vec{v}_{k+1},\end{aligned}$$

where γ (typically between 0.9 and 0.99) is the momentum coefficient that controls how much past gradients influence the current update. This optimizer often accelerates learning in practice by effectively smoothing noisy or rapidly changing gradients.

2.6.3 Nesterov Momentum Optimizer (NMomentum)

Nesterov Momentum, sometimes referred to as *Nesterov's Accelerated Gradient (NAG)*, refines the idea of Momentum by anticipating the next position of the parameters before computing the gradient. Concretely, one computes the gradient at $\vec{\theta} + \gamma\vec{v}$ rather than at

$\vec{\theta}$ only. The updates become:

$$\begin{aligned}\vec{v}_{k+1} &= \gamma \vec{v}_k - \eta \nabla_{\vec{\theta}} E\big(\vec{\theta}_k + \gamma \vec{v}_k\big),\\ \vec{\theta}_{k+1} &= \vec{\theta}_k + \vec{v}_{k+1}.\end{aligned}$$

By 'looking ahead' in the direction of the velocity term, Nesterov Momentum tends to achieve smoother convergence and better performance on problems with numerous local minima or saddle points, which are common in complex quantum simulations.

2.6.4 RMSProp

RMSProp is a gradient-based optimizer that adaptively tunes the learning rate for each parameter by normalizing the gradient through a moving average of its recent magnitudes. This helps address issues of vanishing or exploding gradients, which can be particularly troublesome in variational circuits of moderate or large depth. Its core update equations are:

$$\begin{aligned}E[\nabla^2_{\vec{\theta}}]_k &= \beta\, E[\nabla^2_{\vec{\theta}}]_{k-1} + (1-\beta)\, \nabla_{\vec{\theta}} E(\vec{\theta}_k)^2,\\ \vec{\theta}_{k+1} &= \vec{\theta}_k - \eta\, \frac{\nabla_{\vec{\theta}} E(\vec{\theta}_k)}{\sqrt{E[\nabla^2_{\vec{\theta}}]_k + \epsilon}},\end{aligned}$$

where $0 < \beta < 1$ is a decay factor controlling the smoothing effect, and ϵ is a small constant ensuring numerical stability.

2.6.5 Adagrad

Adagrad is an early approach to adaptive learning rates, designed to handle sparse or highly non-uniform gradients. It individually scales the updates by the inverse square root of the cumulative sum of gradients:

$$\vec{\theta}_{k+1} = \vec{\theta}_k - \frac{\eta}{\sqrt{\sum_{i=1}^{k} \nabla_{\vec{\theta}} E(\vec{\theta}_i)^2 + \epsilon}}\, \nabla_{\vec{\theta}} E(\vec{\theta}_k).$$

This mechanism allows parameters with small but consistent gradients to receive larger updates, which can be helpful in certain quantum chemistry models where specific Hamiltonian terms dominate.

2.6.6 Adam

Adam (Adaptive Moment Estimation) has emerged as one of the most widely used optimizers in machine learning and, increasingly, in quantum algorithms. It combines Momentum-like accumulations of the first moment of gradients (i.e., the mean) with an RMSProp-like treatment of the second moment (i.e., the uncentered variance). The update rules are:

$$\begin{aligned}
\vec{m}_{k+1} &= \beta_1 \vec{m}_k + (1-\beta_1)\nabla_{\vec{\theta}} E(\vec{\theta}_k), \\
\vec{v}_{k+1} &= \beta_2 \vec{v}_k + (1-\beta_2)\nabla_{\vec{\theta}} E(\vec{\theta}_k)^2, \\
\hat{\vec{m}}_{k+1} &= \frac{\vec{m}_{k+1}}{1-\beta_1^{k+1}}, \quad \hat{\vec{v}}_{k+1} = \frac{\vec{v}_{k+1}}{1-\beta_2^{k+1}}, \\
\vec{\theta}_{k+1} &= \vec{\theta}_k - \eta \frac{\hat{\vec{m}}_{k+1}}{\sqrt{\hat{\vec{v}}_{k+1}} + \epsilon},
\end{aligned}$$

where $0 < \beta_1, \beta_2 < 1$ are decay hyperparameters controlling how quickly the estimates of the first and second moments adjust. Adam's blend of adaptive step sizes and momentum often yields robust performance, even when the cost landscape is noisy or irregular, as is typical in quantum simulations.

2.6.7 Quantum Natural Gradient (QNG)

Unlike classical optimizers that rely on Euclidean metrics in parameter space, *Quantum Natural Gradient (QNG)* specifically incorporates the *Fubini–Study* metric, capturing how small changes in the parameters affect the underlying quantum state. By working with a geometry adapted to the quantum manifold, QNG can achieve faster and more reliable convergence in variational circuits. Conceptually, the update rule can be written as:

$$\vec{\theta}_{k+1} = \vec{\theta}_k - \eta\, \mathcal{F}^{-1} \nabla_{\vec{\theta}} E(\vec{\theta}_k),$$

where $\mathcal{F}$ represents the *quantum Fisher information matrix*, a matrix encoding the local geometry of the parameterized state. Computing $\mathcal{F}$ can be more demanding than classical gradients, but for many quantum chemistry or condensed-matter applications, the improved efficiency justifies this added cost.

2.6.8 Importance of Optimizers in Quantum Simulation

Optimizers bridge the gap between quantum hardware and classical processing by iteratively refining the variational parameters to minimize the expectation value of the Hamiltonian. They must contend with challenges specific to quantum simulation, such as measurement noise, limited qubit counts, and complex cost landscapes characterized by local minima and barren plateaus. Properly choosing and tuning the optimizer is paramount to achieving accurate, resource-efficient simulations. By harnessing the distinctive advantages of adaptive and momentum-based methods—as well as more specialized quantum-aware techniques like QNG—one can significantly improve the speed and reliability of variational algorithms, thereby pushing the capabilities of quantum simulation closer to practical applications in molecular modeling.

CHAPTER 3

Methodology / project development

This chapter details the methodology used to execute the project, providing a clear and concise description of the approaches and techniques implemented to ensure replicability and academic rigor. It not only covers the research methods and measurement techniques but also delves into specific aspects of software development and project structuring. Whether the project involves computational modeling, algorithm implementation and software optimization, this section explains how each component contributes to the overall objectives.

Additionally, the chapter provides justifications for selecting specific approaches over alternatives. For instance, the **PennyLane** framework was chosen over **Qiskit** for quantum simulations due to its robust documentation and practical examples in molecular simulations. The adoption of the **Variational Quantum Eigensolver (VQE)** algorithm was motivated by its compatibility with Noisy Intermediate-Scale Quantum (NISQ) devices. Parallelization strategies were implemented to enhance computational efficiency and reduce execution times.

The project follows a modular structure that facilitates scalability and simplifies the integration of new functionalities. The codebase is organized into configuration files, main execution scripts, and core computational modules. Furthermore, the adaptive construction of the *ansatz* and operator selection processes are described, highlighting how these techniques improve the accuracy and efficiency of quantum simulations.

Finally, the chapter addresses the limitations of the chosen methodologies and the strategies applied to mitigate these challenges. These include managing framework stability issues, computational resource constraints, and optimization convergence difficulties. By transparently discussing the strengths and weaknesses, this section presents a balanced view of the development process, emphasizing its reliability and robustness.

3.1 Tools and Frameworks Selection

To achieve the objectives of our project, the first crucial step was to select the framework to be used throughout the development process. This decision was essential, as it directly influenced the progress and success of the project.

To make the decision on which framework to use, we compared the documentation of the two quantum simulation frameworks available in the market: *PennyLane* and *Qiskit*. These are the most comprehensive frameworks with similar features available at the time of creating this project. After reviewing the documentation, we ultimately chose to use *PennyLane* for two reasons.

The first reason was the amount of documentation related to quantum simulation. Once we started looking into how others were using these resources, we realized that in the field of molecular simulation, the existing documentation—both theoretical and especially practical—was substantially greater. This provided us with more examples to begin developing our project and a more extensive theoretical background to understand the concepts we were working with.

The second reason for our choice was the frequent major changes implemented by *Qiskit*. We realized that while *Qiskit* is a tool that promises to be very good, it has historically undergone significant structural changes. For these reasons, this project has been developed using the *PennyLane* framework.

3.1.1 Version Control

Git was employed for version control, enabling detailed tracking of code changes and ongoing collaboration with project supervisors. Initially, a single branch was used for development and exploration. Once a stable version was established, branches were created for testing and adding new features. The first branches were dedicated to different interface versions, each refined to ensure consistent performance across all interfaces. Ultimately, only the most suitable interface adjustments were merged back into the main branch.

3.2 Project Structuring

After selecting the interface and implementing the initial version of the code, we reorganized the project to achieve a more modular structure. This revised organization not only makes it easier to add new functionalities but also ensures that the project can handle higher levels of complexity. Below, we present the structure of the project and the functionality of each directory and file.

3.2.1 Code Organization

```
                    quantum_simulation_project/
config/
     config_functions.py: Configuration functions for the project.
     molecules.json: JSON file containing molecular data.
main.py: The main entry point for the program.
modules/
     ansatz_preparer.py: Quantum ansatz preparation.
     hamiltonian_builder.py: Molecular Hamiltonian construction.
     molecule_manager.py: Molecular data management.
     opt_mol.py: End-to-end molecular optimization.
     optimizer.py: Optimization algorithms.
     visualizer.py: Visualization tools.
temp_results_autograd/
     energy_evolution.png: Graph of energy convergence.
     filtered_report_autograd.txt: Filtered results report.
     final_geometries_3D.png: Final 3D geometries.
     nuclear_coordinates.png: Nuclear coordinates visualization.
     output.txt: Program output log.
     profile_output_autograd.txt: Autograd profiling output.
test/: Directory for tests.
```

3.2.2 Main Directory

- `main.py`: Central entry point of the program. It initializes the process by selecting molecules, configuring the optimizer, and setting up the ansatz. It also manages the optimization workflow, handles result storage, and produces comprehensive reports. Profiling tools evaluate computational performance.

3.2.3 `config/` Directory

- `config_functions.py`: Handles project configuration. This includes loading molecular data, selecting optimization algorithms, and setting initial parameters such as ansatz type and convergence tolerance. The module also allows adding custom molecules and organizing saved results.
- `molecules.json`: A structured JSON file containing information about molecules, including atomic symbols, coordinates, charges, and spin multiplicities.

3.2.4 `modules/` Directory

Core computational logic resides here:

- `ansatz_preparer.py`: Implements quantum circuit construction (ansätze) for both adaptive and traditional methods. Includes the UCCSD ansatz (single and double excitations) and hardware-efficient ansatzes featuring multiple circuit layers.

- `hamiltonian_builder.py`: Constructs the molecular Hamiltonian, a fundamental component of quantum simulations. Calculates Hartree-Fock reference states and can extract exact energy values from the Hamiltonian matrix.
- `molecule_manager.py`: Initializes molecules by processing atomic symbols, initial coordinates, and configuration parameters such as charge and multiplicity. Also computes important properties like the number of electrons and orbitals.
- `optimizer.py`: Contains optimization algorithms (e.g., Adam, QNG, RMSProp). Integrates parameter updates and nuclear coordinate adjustments in a unified optimization framework.
- `opt_mol.py`: Orchestrates the complete molecular optimization pipeline. Brings together Hamiltonian construction, molecule management, optimization routines, and result visualization.
- `visualizer.py`: Offers visualization tools for energy convergence and molecular geometries. Generates detailed graphical outputs in both linear and logarithmic scales.

3.2.5 `temp_results_autograd/` Directory

Contains intermediate results generated during simulations:

- `energy_evolution.png`: Graph of energy convergence over iterations.
- `nuclear_coordinates.png`: Visualization of nuclear coordinates during optimization.
- `filtered_report_autograd.txt`: Filtered report of relevant profiling metrics.
- `output.txt`: Primary output log of the program.

3.3 Implementation of the VQE

Before delving into how molecular energy optimization has been implemented, it is crucial to first detail the methodology employed for optimizing the system parameters. This process was conducted using the *Variational Quantum Eigensolver* (VQE), which was selected as the primary method to estimate the ground state energy of the quantum system under study.

The VQE algorithm integrates limited quantum processing, characterized by measurements and shallow quantum circuits, with classical optimization techniques. Its selection is grounded on the following justifications:

- **Suitability for NISQ devices:** VQE is particularly well-suited for noisy intermediate-scale quantum (NISQ) devices, as it requires circuits of relatively low depth.
- **Flexible Ansatz:** It allows the use of various adaptive variational ansätze that capture essential electronic correlations.
- **Direct coupling to classical optimizers:** The VQE cost function (the expected energy) can be minimized with a wide range of classical methods, making it easy to experiment with different optimizers.

The core principle of VQE is the variational theorem, which guarantees that the expected energy of the ansatz is always an upper bound to the true ground state energy. By optimizing the ansatz parameters, the algorithm progressively approaches the actual energy minimum. We have already explained the concept of VQE in the state of the art chapter; now we will explain how we have implemented it in our project and how we have integrated it.

Principle of VQE:

The VQE is based on the variational principle, which states that the expected energy of any approximate state $|\psi(\theta)\rangle$ is always greater than or equal to the real ground state energy E_0:

$$E(\theta) = \langle\psi(\theta)|H|\psi(\theta)\rangle \geq E_0$$

We have already discussed this concept, but it is necessary to emphasize it as it is the foundation of the entire algorithm. The idea is to find the parameters θ that minimize the expected energy, thereby approaching the real value of the ground state energy.

Next, we will explore the implementation of the VQE within our project, breaking down its key components. Each element plays a crucial role in ensuring the algorithm's accuracy and efficiency: the molecular Hamiltonian defines the energy landscape, the ansatz captures electronic correlations through parameterized quantum circuits and the cost function evaluates the expected energy, guiding the optimization. This section outlines how each of these components was designed and integrated to maximize performance and precision.

3.3.1 Hamiltonian Construction Process

1. **Definition of Molecular Geometry:**

   First of all, it is necessary to define the molecular geometry of the system to be studied. This information includes the atomic symbols and the initial coordinates of the nuclei. In our project, this data is stored in a JSON file, which is loaded and processed to initialize the molecule. However, custom molecules can also be added directly in the code.

This part of the code provides the user with the ability to select the molecule to be simulated, allowing them to choose between the predefined molecules in the JSON file or add a new one. The `from_user_input` function loads the molecular information and initializes it, preparing it for simulation.

2. **Hamiltonian Construction:**

Once the molecular geometry is defined, the next step is to construct the system's Hamiltonian. This Hamiltonian represents the total energy of the system and is fundamental for quantum simulation. In our project, the Hamiltonian is constructed using the `build_hamiltonian` function, which transforms the electronic Hamiltonian from its second-quantized form into a qubit-based representation. This implementation is relatively straightforward as it relies on PennyLane's `molecular_hamiltonian` function, which generates the Hamiltonian from the atomic symbols, coordinates, and other system parameters.

Hamiltonian Build

```python
def build_hamiltonian(x, symbols, charge=0, mult=1, basis_name='sto-3g'):
    x = np.array(x)
    coordinates = x.reshape(-1, 3)
    hamiltonian, qubits = qml.qchem.molecular_hamiltonian(
        symbols, coordinates, charge=charge, mult=mult, basis=basis_name
    )
    h_coeffs, h_ops = hamiltonian.terms()
    h_coeffs = np.array(h_coeffs)
    return qml.Hamiltonian(h_coeffs, h_ops)
```

Note: A basis set, such as `sto-3g`, is chosen to represent atomic orbitals. This predefined set of basis functions simplifies the simulation while retaining sufficient accuracy for many molecular systems.

Apart from transforming the electronic Hamiltonian, initially expressed in its second-quantized form, into a qubit-based representation suitable for quantum computation, this function also allows the inclusion of user-defined parameters, such as the net molecular charge and the spin multiplicity, providing flexibility to simulate a wide range of electronic states. This feature is particularly important for accurately representing systems with different charge states and spin configurations.

Furthermore, it optionally supports the definition of an active space, allowing the focus to be limited to the most relevant orbitals and electrons, thus optimizing resource usage without sacrificing significant accuracy.

3.3.2 Adaptive Ansatz Construction and Operator Selection

For the constructioon of the ansatz, we use the adaptive ansatz construction builds upon the conventional variational approach by strategically selecting only those excitations that offer the most significant energy reductions. Instead of starting from a large, fixed set of parameters, the algorithm begins with the Hartree-Fock state and incrementally introduces new excitations based on their calculated impact on lowering the system's energy. This methodology provides both theoretical and practical advantages in handling the complexity of the solution space.

The selection process begins with a predefined *operator pool,*composed of single and double excitation operators relevant to the molecular system. At the start of the procedure, no variational parameters are assigned, and the system is initialized in the reference Hartree-Fock state. At each iteration, the algorithm evaluates the energy gradients associated with adding each operator from the pool.

Below we present the main steps of the adaptive ansatz construction and operator selection process, all implemented on the `ansatz_preparer.py` file:

1. **Gradient Calculation:** For every candidate operator $\hat{O}_i$ in the pool, the partial derivative of the energy with respect to the parameter controlling $\hat{O}_i$ is computed. This step identifies how sensitive the energy is to introducing that particular excitation. In our project this functionality is implemented in the `compute_operator_gradients` function.

Gradient Calculation

```python
def compute_operator_gradients(operator_pool, selected_excitations,
     params, hamiltonian, hf_state, dev, spin_orbitals, ansatz_type
    ="uccsd"):
    gradients = []
    for gate_wires in operator_pool:
        param_init_autograd = np.array(0.0, requires_grad=True)

        @qml.qnode(dev, interface="autograd")
        def circuit_with_gate(param):
            prepare_ansatz(params, hf_state, selected_excitations,
                spin_orbitals, ansatz_type=ansatz_type)
            if len(gate_wires) == 2:
                qml.SingleExcitation(param, wires=gate_wires)
            elif len(gate_wires) == 4:
                qml.DoubleExcitation(param, wires=gate_wires)
            return qml.expval(hamiltonian)

        grad_fn_autograd = qml.grad(circuit_with_gate, argnum=0)
        grad = grad_fn_autograd(param_init_autograd)
        gradients.append(np.abs(grad))

    return gradients
```

2. **Operator Ranking and Filtering:** All candidate excitations are ranked according to the absolute value of their gradients. Operators that produce negligible energy changes are discarded, while those offering substantial decreases are selected for inclusion. The `select_operator` function implements this filtering process.

Operation Ranking

```python
def select_operator(gradients, operator_pool, convergence):
    if len(gradients) == 0 or np.all(np.isnan(gradients)):
        return None, None

    max_grad_index = np.argmax(gradients)
    max_grad_value = gradients[max_grad_index]

    if max_grad_value < convergence:
        return None, None
    selected_gate = operator_pool[max_grad_index]
    return selected_gate, max_grad_value
```

3. **Incremental Ansatz Growth:** The selected operator(s) is then added to the ansatz. A new parameter is introduced and optimized, increasing the dimensionality of the parameter space *only where it matters*. This targeted expansion ensures that each additional parameter contributes meaningfully to lowering the energy. The incremental ansatz is implemented de la siguiente manera:

Operation Ranking

```python
def prepare_ansatz_uccsd(params, hf_state, selected_excitations,
    spin_orbitals):
    qml.BasisState(hf_state, wires=range(spin_orbitals))
    for i, exc in enumerate(selected_excitations):
        if len(exc) == 2:
            qml.SingleExcitation(params[i], wires=exc)
        elif len(exc) == 4:
            qml.DoubleExcitation(params[i], wires=exc)
```

4. **Pool Update and Iteration:** After adding the chosen operators, the process repeats. The operator pool is re-examined at subsequent steps, but it now excludes previously chosen operators unless they are included as parameterized parts of the ansatz. Over multiple iterations, the ansatz evolves adaptively, honing in on the

most relevant subset of excitations.

Below, we can observe a simplified code snippet, consistent with the project's implementation, showcasing the adaptive operator selection process:

Adaptive Operator Selection

```python
gradients = compute_operator_gradients(operator_pool,
    selected_excitations, params, hamiltonian, hf_state, dev,
    spin_orbitals)
selected_gate, max_grad_value = select_operator(gradients, operator_pool,
     convergence_threshold)
if selected_gate:
    selected_excitations.append(selected_gate)
    params = np.append(params, 0.0)  # Add new parameter for the chosen
        operator
    print(f"Added operator {selected_gate} with gradient {max_grad_value
        :.5e}")
else:
    print("No significant operators found. Convergence or local minimum
        reached.")
```

Adaptive Ansatz Benefits

In summary, this code uses the `compute_operator_gradients` function to evaluate each operator's gradient, while the `select_operator` function applies a filtering criterion based on a defined `convergence_threshold`. Only the most promising excitation is incorporated into the ansatz at each step, ensuring a controlled and meaningful expansion of the parameter space.

In numerical experiments, this targeted approach has demonstrated:

- **Faster Convergence:** Fewer parameters are introduced at each stage, allowing the optimizer to quickly reduce the energy without wading through irrelevant configurations.

- **Lower Resource Consumption:** By refining the search space, the quantum circuits remain relatively shallow, and classical optimization routines require fewer evaluations.

- **Scalability:** As molecular systems grow in complexity, the adaptive approach helps mitigate the exponential growth in parameter number, making it more feasible to handle larger systems within similar computational budgets.

3.3.3 Cost Function Definition

With the ansatz defined, the next step is to establish a cost function that evaluates the expected energy of the system given a set of parameters θ. In our implementation, this cost function is defined within `update_parameters_and_coordinates` and calculates the expected value of the molecular Hamiltonian:

Definition of the Cost Function

```python
@qml.qnode(dev, interface=interface)
def cost_fn(params):
    prepare_ansatz(params, hf_state, selected_excitations, spin_orbitals)
    return qml.expval(hamiltonian)
```

In our implementation, `prepare_ansatz` serves as an auxiliary function that enables the selection of the desired ansatz for implementation. This flexibility has also allowed us to compare the effectiveness of the UCCSD ansatz against other ansätze. Below is the function that facilitates the selection of the ansatz to be used:

Ansatz Selection

```python
def prepare_ansatz(params, hf_state, selected_excitations, spin_orbitals,
     ansatz_type="uccsd", num_layers = 10):
    if ansatz_type not in ANSATZ_MAP:
        raise ValueError(f"Ansatz type '{ansatz_type}' is not recognized.
            Available: {list(ANSATZ_MAP.keys())}")

    ansatz_fn = ANSATZ_MAP[ansatz_type]

    if ansatz_type == "uccsd":
        ansatz_fn(params, hf_state, selected_excitations, spin_orbitals)
    else:
        ansatz_fn(num_layers,params, hf_state, [], spin_orbitals)
```

This function is essential for evaluating $E(\theta)$. By calculating the expected value of the Hamiltonian, we can quantify how close our approximate state is to the true ground state.

3.4 Mixed Optimization Strategy

In this work, both the variational parameters θ (electronic) and the nuclear coordinates $\mathbf{X}$ (geometric) are refined within a single iterative loop. This coupled approach ensures that each electronic update reflects the current molecular geometry, while each geometric update leverages the most accurate electronic wavefunction available. By jointly optimizing θ and $\mathbf{X}$, the algorithm can converge more efficiently to a physically meaningful global minimum.

3.4.1 Rationale for a Coupled Scheme

Traditional sequential approaches often optimize electronic parameters at a fixed geometry, then update the geometry using the finalized electronic structure. Such a split workflow can lead to unnecessary iterations and less-precise intermediate results. Because the electronic distribution and the molecular geometry are inherently interdependent, we opt to update both simultaneously, thereby reducing computational overhead and converging more smoothly to the system's equilibrium configuration.

3.4.2 Iterative Optimization Steps

The key steps of the coupled optimization process, implemented in the *run_optimization_uccsd* function within the `optimizer.py` file, are described below:

1. **Initialization:** Firts of all, we define the initial geometry $\mathbf{X}_0$, variational parameters θ_0, and other required structures.

Initialization

```python
import pennylane as qml
from pennylane import numpy as np

# In run_single_optimizer (lines near 290+ in the code):
params = np.array([], requires_grad=True)  # Starting with empty
    parameters
operator_pool_copy = operator_pool.copy()
selected_excitations = []
x = x_init.copy()  # Copy of the initial geometry

# Set up the environment for optimization:
exact_energy = compute_exact_energy(symbols, x_init, charge, mult,
    basis_name)
hf_state = generate_hf_state(electrons, spin_orbitals)
dev = qml.device("default.qubit", wires=spin_orbitals)
```

2. **Hamiltonian Recalculation:** Then, at each iteration, the molecular Hamiltonian is rebuilt for the current geometry $\mathbf{X}$. This step ensures that the energy evaluation remains accurate and up-to-date with the latest nuclear configuration on each optimization cycle.

Hamiltonian Recalculation

```python
# In run_optimization_uccsd (lines near 124+):
for iteration in range(max_iterations):
    # Rebuild the Hamiltonian for the current geometry 'x'
    hamiltonian = build_hamiltonian(x, symbols, charge, mult,
        basis_name)

    # Additional iteration logic follows:
```

3. **Electronic Update via Operator Gradients:** The text is clear, but it can be slightly refined for better readability and grammatical correctness. Here's the revised version:

   The next step is to compute the energy gradient with respect to a pool of candidate excitation operators. We select the operator that yields the largest energy decrease and add it to the ansatz. This strategy expands the variational parameter space only in directions that significantly reduce the energy.

Electronic Update

```python
# Same loop in run_optimization_uccsd:
gradients = compute_operator_gradients(
    operator_pool_copy,
    selected_excitations,
    params,
    hamiltonian,
    hf_state,
    dev,
    spin_orbitals,
    ansatz_type="uccsd"
)

selected_gate, max_grad_value = select_operator(gradients,
    operator_pool_copy, CONV)
if selected_gate is None:
    print("No operators selected. Stopping optimization for uccsd."
        )
    break

selected_excitations.append(selected_gate)
params = np.append(params, 0.0)  # Add a new variational parameter
params = np.array(params, requires_grad=True)
print(f"Added operator {selected_gate} with gradient {
    max_grad_value:.5e}")
```

4. **Geometric Update via Finite Differences:** On the same iteration, we update the geometry by numerically approximating $\nabla_{\mathbf{X}} E(\theta, \mathbf{X})$through small perturbations to each coordinate. The geometry is then updated as follows:

$$\mathbf{X} \leftarrow \mathbf{X} \; - \; \alpha \, \nabla_{\mathbf{X}} E(\theta, \mathbf{X}),$$

   where α is a suitably chosen learning rate. This technique avoids overly complex gradient calculations while remaining flexible and straightforward to implement.

Geometric Update

```
# In update_parameters_and_coordinates (lines near 59+):
grad_x = compute_nuclear_gradients(
    params, x, symbols, selected_excitations, dev,
    hf_state, spin_orbitals, interface, charge, mult, basis_name
)

# Apply the update:
x = x - learning_rate_x * grad_x
```

5. **Convergence Checks:** Then, we impose strict thresholds on both the change in total energy and the geometric displacements. Once these criteria are satisfied, the geometry is deemed optimized and stable, and the refinement process is terminated.

Convergence Checks

```
# In update_parameters_and_coordinates (lines near 52+):
energy = np.real(energy)
if check_convergence(energy, prev_energy, recent_diffs):
    print(f"Convergence reached updating parameters and coordinates
        : Energy difference < {CONV}")
    converged = True
    prev_energy = energy
    # Code returns early, finalizing this substep
```

6. **Visualization and Termination:** Finally, we track the evolution of energy and geometry at every iteration, providing immediate graphical feedback (e.g., energy vs. iteration plots). This step helps identify convergence, reveals unexpected behaviors early, and confirms when additional optimization no longer benefits the system.

Visualization and Termination

```
# Example of final printout and logging in run_optimization_uccsd:
print(f"Iteration {iteration + 1}, Energy = {current_energy:.8f} Ha
    , Max Gradient = {max_grad_value:.5e}")
```

```python

# After all iterations or once convergence is reached:
print(f"Total optimization time (uccsd): {total_time:.2f} seconds")
print(f"Final energy with {optimizer_name} (autograd) = {
    final_energy:.8f} Ha")
print(f"Difference from exact (FCI) energy: {diff:.8e} Ha")

# Geometry and circuit details are saved or printed:
for i, atom in enumerate(symbols):
    atoms_coords.append([atom, final_x_np[3*i], final_x_np[3*i+1],
        final_x_np[3*i+2]])
print(tabulate(atoms_coords, headers=["Symbol", "x (A)", "y (A)", "
    z (A)"], floatfmt=".6f"))
```

3.4.3 Efficiency of the Coupled Strategy

By refining θ and $\mathbf{X}$ concurrently, each electronic update leverages a geometry already progressing toward equilibrium. Likewise, every geometric move reflects the latest improvements to the electronic wavefunction. This synergy minimizes redundant calculations and avoids suboptimal solutions, typically leading to faster, more stable convergence compared to the conventional, decoupled approach.

3.5 Parallelization of Executions

One of the main improvements implemented in the project to accelerate execution and provide greater flexibility in our simulations has been parallelization. To achieve this, it was necessary to adapt the code so that simulations could be executed concurrently. Below, the process followed to enable this functionality is detailed.

3.5.1 User Input Management and System Configuration

To allow the user to configure the different types of simulations, a configuration file was incorporated in the `config/` directory, named `config_functions.py`. This file defines variables that allow specifying, among other things, the type of molecule, the optimizer, and the *ansatz*:

User Input Management

```python
parser = argparse.ArgumentParser(description='Quantum simulation of
    molecules using VQE.')
parser.add_argument('--molecule', type=str, nargs='+', help='Molecule(s)
    to simulate.')
```

```
parser.add_argument('--optimizer', type=str, nargs='+', help='Optimizers
    to use (Adam, Adagrad, etc.).')
parser.add_argument('--stepsize', type=float, nargs='+', default=[0.4],
    help='Optimizer step size(s).')
parser.add_argument('--ansatz', type=str, nargs='+', help='Ansatz to use
    (e.g. uccsd, vqe_classic).')
args = parser.parse_args()
```

Before starting each simulation, two key lists are constructed:

- One with the optimizers to be used for each execution.
- Another with the additional parameters (the type of *ansatz*, the number of layers, the number of optimizations, etc.).

The `build_optimizers` function automatically generates the optimizers and organizes these parameters:

Generación de optimizadores

```
def build_optimizers(args, ansatz_list, optimizer_map, predefined_steps):
    optimizers, new_ans = {}, []
    if args.all_optimizers:
        all_opts = list(optimizer_map.keys())
        user_steps = (args.stepsize != [0.4] or len(args.stepsize) > 1)
        for opt in all_opts:
            steps_for_opt = args.stepsize if user_steps else [
                predefined_steps[opt]]
            for step in steps_for_opt:
                for n in args.opt_step:
                    for ans_type, layer in ansatz_list:
                        name = f"{opt}_{step}_{ans_type}_{layer}layers_{n
                            }steps"
                        optimizers[name] = optimizer_map[opt](stepsize=
                            step)
                        new_ans.append((ans_type, layer, n))
    elif args.optimizer:
        for opt in args.optimizer:
            if opt not in optimizer_map:
                print(f"Error: Optimizer '{opt}' not recognized.")
                sys.exit(1)
            for step in args.stepsize:
                for n in args.opt_step:
                    for ans_type, layer in ansatz_list:
                        name = f"{opt}_{step}_{ans_type}_{layer}layers_{n
                            }steps"
                        optimizers[name] = optimizer_map[opt](stepsize=step)
                        new_ans.append((ans_type, layer, n))
    else:
        # Default value if neither --optimizer nor --all_optimizers is specified
        for step in args.stepsize:
            for n in args.opt_step:
                for ans_type, layer in ansatz_list:
                    name = f"NMomentum_{step}_{ans_type}_{layer}layers_{n}steps"
                    optimizers[name] = NesterovMomentumOptimizer(stepsize=step)
                    new_ans.append((ans_type, layer, n))
    return optimizers, new_ans
```

3.5.2 Parallelization of Execution with Multiple Optimizers

After generating the optimizers and their corresponding configurations, the parallel execution process is invoked. This approach distributes each simulation across different processes using `ProcessPoolExecutor`, thereby leveraging multiple CPU cores to significantly accelerate computation time:

Paralelización de procesos

```
with concurrent.futures.ProcessPoolExecutor() as executor:
    futures = []
    cont = 0
    for optimizer_name, opt in optimizers.items():
        if cont < len(ansatz_list):
            ans_type, layers, nsteps = ansatz_list[cont]
        else:
            ans_type, layers, nsteps = ("uccsd", 0, 10)
        cont += 1
        futures.append(
            executor.submit(
                run_single_optimizer,
                optimizer_name, opt, ans_type, layers, nsteps, symbols, x_init, electrons, spin_orbitals, charge,
                mult, basis_name, hf_state, dev, operator_pool, exact_energy, results_dir
            )
        )
```

In this way, each optimizer is executed independently, allowing for the maximum utilization of available hardware resources. This accelerates the simulation process and provides greater flexibility in experimenting with different configurations.

3.5.3 Compilation of Results and Cleanup of Temporary Files

After completing the execution of parallel processes, several key steps are carried out to unify results, clean up temporary files, and generate the final results. Each step is detailed below along with the corresponding code.

Creation and Execution of Parallel Processes

Parallel processes are created using `ProcessPoolExecutor`. For each configured optimizer, simulations are submitted as tasks to the executor, and the corresponding *futures* are stored. Once they complete, the results are collected in the `interface_results` dictionary.

Creation and Execution of Parallel Processes

```

# Collect results when processes finish
for future in concurrent.futures.as_completed(futures):
    optimizer_name, data = future.result()
    interface_results[optimizer_name] = data
```

Unification of Results into a Single File

To centralize the simulation information, the contents of individual output files (`output_{optimizer_name}.`
are combined into a single file named `combined_output.txt`.

Unification of Results into a Single File

```
combined_output_path = os.path.join(results_dir, "combined_output.txt")
with open(combined_output_path, "w", encoding="utf-8") as combined_out:
    for optimizer_name in optimizers.keys():
        output_file = os.path.join(results_dir, f"output_{optimizer_name
            }.txt")
        if os.path.exists(output_file):
            with open(output_file, "r", encoding="utf-8") as f:
                content = f.read()
            combined_out.write(f"=== Optimizer: {optimizer_name} ===\n")
            combined_out.write(content + "\n")
```

Deletion of Temporary Files

Once the individual data has been centralized, the temporary output files are deleted to reduce disk space usage and clean the results directory.

Deletion of Temporary Files

```python
for optimizer_name in optimizers.keys():
    output_file = os.path.join(results_dir, f"output_{optimizer_name}.txt
        ")
    if os.path.exists(output_file):
        os.remove(output_file)
```

Generation of Final Results

The final results, such as the optimized energy, differences from the exact energy, and final molecular geometries, are presented to the user. Additionally, execution times and corresponding quantum circuits are visualized.

Generation of Final Results

```python
print("=== Total Optimization Times ===\n")
for optimizer_name in optimizers.keys():
    final_energy = interface_results[optimizer_name]["final_energy"]
    exact_energy_ref = interface_results[optimizer_name]["
        exact_energy_reference"]
    diff = final_energy - exact_energy_ref if final_energy is not None
        else None
    if final_energy is not None:
        print(f"Final energy with {optimizer_name} = {final_energy:.8f}
            Ha")
        print(f"Difference from exact (FCI) energy: {diff:.8e} Ha\n")
    else:
        print(f"No final energy obtained with {optimizer_name}\n")

    total_time = interface_results[optimizer_name]["execution_times"].get
        ('Total Time', 0)
    print(f"Optimizer: {optimizer_name}, Time: {total_time:.2f} seconds")
```

In this way, the complete workflow allows:

1. Executing processes in parallel and collecting their results.
2. Unifying the generated data into a single output file.
3. Cleaning up temporary files to maintain an organized directory.

4. Presenting the final results in a clear and detailed manner.

CHAPTER 4

Results

This chapter should encompass your data analysis and findings. Additionally, include relevant tables, figures, and citations to support your results and interpretations. Here is a suggested list of topics to discuss:

4.1 Interface Comparison

During the development of this project, various experiments were conducted to optimize the performance of a quantum molecular simulator. In this context, the choice of the interface for calculating cost functions is crucial, as these functions must be optimized to obtain the optimal state and geometry of each molecule. Typically, the *JAX* interface is the most widely used due to its GPU acceleration capabilities, which generally provide greater efficiency and speed in searching for the minimum of the cost function.

However, when comparing two identical implementations—varying only the calculation interface—we observed a surprising result: the *JAX*-based interface, which was executed on a GPU, was slower than the *autograd*-based interface, which ran on a CPU. To confirm that this was not a coding error, we repeated the experiments on different machines, obtaining the same result. For this reason, we decided to continue with the *autograd* interface due to its greater speed in our specific implementation.

4.1.1 Optimization and Timing Logging

To verify the performance differences between both interfaces, the same optimization was executed while varying only the interface. During these simulations, the execution times of the different functions in the code were recorded, with their values shown in Table 4.1.

Function	[Li, H] _autograd_GD	[Li, H] _jax_GD	[O, H, H] _autograd_GD	[O, H, H] _jax_GD	[H, H] _autograd_GD	[H, H] _jax_GD
Iteration 1	1246.7627	6251.3362	6942.21696	39003.89009	14.6908	40.5485
Iteration 2	1244.0321	6284.9812	6935.09353	40652.7751	14.7824	36.2979
Iteration 3	1247.4399	6348.2470	6920.68571	40386.29868	14.9931	38.6236
Iteration 4	1245.7256	6351.6437	6942.60873	40128.31419	15.0694	39.1362
Iteration 5	1244.8591	6349.5099	6965.70663	40657.74473	15.1512	40.6186
Total Time	6228.8195	31585.7475	34706.3116	200829.0866	74.6870	195.2551
build_hamiltonian	29.1349	30.3407	78.4744	85.7532	0.4934	0.5329
compute_operator_gradients	1533.0319	17497.4381	12563.3726	113792.7167	0.6313	11.9006
update_parameters_and_coordinates	4666.6385	14056.6795	22064.4153	86946.6021	73.5594	182.5271

Table 4.1: *Execution times for different molecules and interfaces using Gradient Descent.*

Figure 4.1 shows how the execution time evolves over the iterations for each molecule and type of interface. It is evident that, in all cases, the *autograd*-based interface offers lower computation times than the *JAX*-based interface.

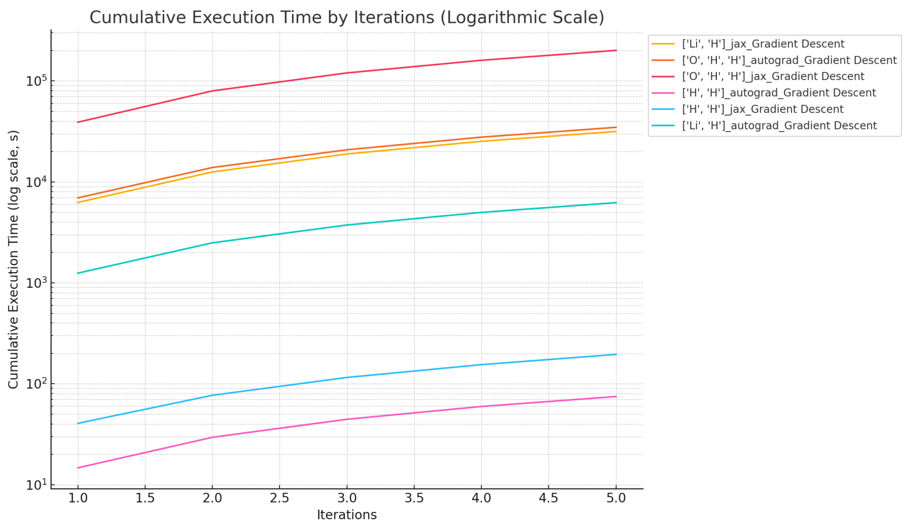

Figure 4.1: *Execution time of different molecules per iteration in the simulation.*

Comparative Performance Analysis

To evaluate the performance of both interfaces in more detail, a table was created showing the percentage increase in execution time of *JAX* compared to *autograd*, as seen in Table 4.2.

Metric	LiH	H_2	H_2O	Mean
Total Time	80.28%	82.72%	61.75%	74.92%
build_hamiltonian	3.97%	8.49%	7.42%	6.63%
compute_operator_gradients	91.24%	88.96%	94.70%	91.63%
update_parameters_and_coordinates	66.80%	74.62%	59.70%	67.04%

Table 4.2: *Comparison of execution times between JAX and autograd interfaces for different molecules.*

On average, it was observed that the *JAX* interface exhibits a 74.92% higher total execution time than the *autograd* interface. Additionally, it is interesting to note that as the complexity of the molecule increases (with a greater number of atoms), the penalty percentage of *JAX* tends to decrease. This behavior suggests that, in larger-scale problems, GPU acceleration could become more competitive, although it does not manage to outperform *autograd* in this implementation.

4.1.2 Computation Time per Function

For a higher level of detail, the computation time was also measured for each part of the code where the interface change is introduced. Figure 4.2 shows the accumulated execution times in the main stages of the algorithm.

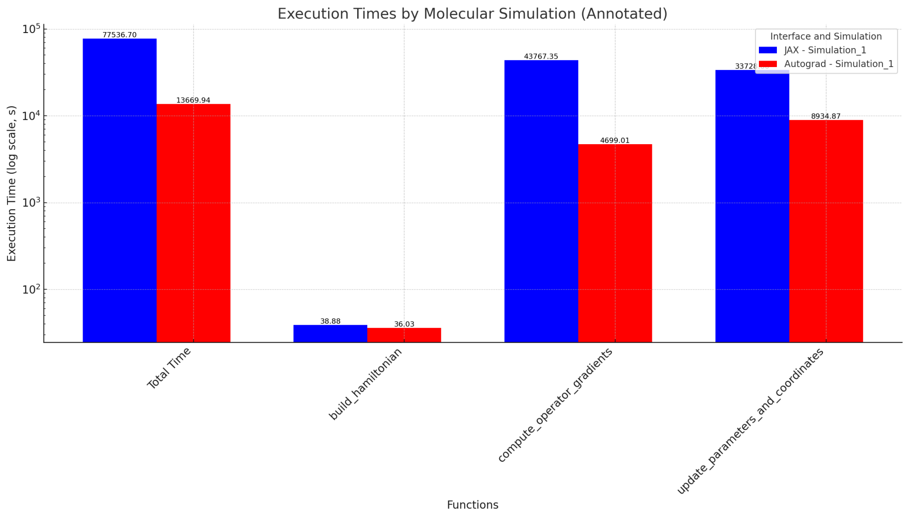

Figure 4.2: *Execution time in different parts of the code.*

The same pattern is maintained in all functions: the *JAX* interface records higher execution times than *autograd*. In particular, the gradient computation part `compute_operator_gradients` increases its execution time by 91.68% when using *JAX*. This difference is largely attributed to the overhead caused by data transfer between the CPU and GPU, especially when *PennyLane* does not fully support generating the molecule's Hamiltonian directly on the GPU.

On the other hand, the function `update_parameters_and_coordinates`, responsible for performing the molecular geometry and parameter optimization step, also shows a 67.04% increase when using *JAX*. Nevertheless, it is worth highlighting that as the problem grows in complexity, the *JAX* interface gains some relative efficiency in gradient calculation; however, the time saved through GPU acceleration is offset by the continuous data transfer between CPU and GPU throughout the iterations.

4.1.3 Conclusions

Based on the obtained results, the *autograd* interface demonstrated superior performance in terms of speed for our implementation of the quantum molecular simulator. Although the GPU is usually advantageous in larger-scale problems, the data transfer overhead and the lack of full support for Hamiltonian generation within the GPU reduced the efficiency of *JAX*. For this reason, we ultimately chose to use the *autograd* interface for the final implementation of the quantum molecular simulator.

4.2 Ansatz Comparison

One of the most important modifications that has significantly affected our code and its functionality has been the choice of the Ansatz. Our proposal has been to implement UCCSD, an Ansatz typically used for this type of simulation, as it enhances the simulation performance by achieving higher efficiency. The efficacy of this type of Ansatz has already been demonstrated, showing how it can improve simulation performance by producing more optimal quantum circuits without the need to create a specific Ansatz for the molecule being simulated. It is a fact that for each optimizer configuration and for each different molecule simulation, there exists an optimal quantum circuit that achieves the best performance. However, since our objective is to develop a program that can simulate various molecules with maximum performance, we observe that the best option is UCCSD. To illustrate how our simulation performance is improved, we have generated Ansätze with different levels of depth and compared their performance with that of a UCCSD Ansatz. We have simulated various configurations of classical Ansätze, and in all cases, the UCCSD Ansatz has achieved better performance. More complex and molecule-specific Ansätze could be tested, but it is unlikely that another type of Ansatz would outperform UCCSD in terms of performance improvement.

Below is a simulation with different Ansatz depths and varying numbers of iterations obtained directly from the simulation.

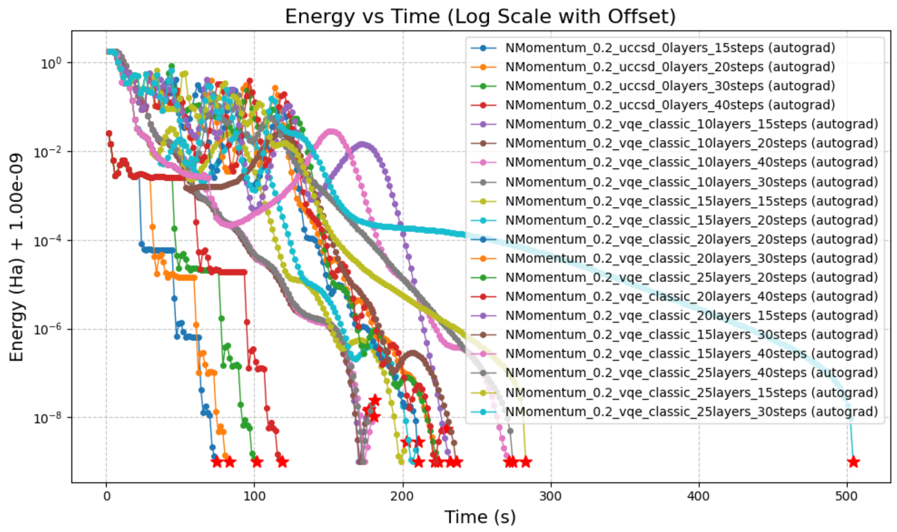

Figure 4.3: *Energy vs. Time for different Ansätze and iterations.*

It is observed that the UCCSD Ansatz achieves the best performance in all simulations, regardless of the number of optimizations performed for each iteration. For greater clarity of the results, a simulation was conducted with only a single number of optimizations per iteration, and the performance of the different Ansätze was compared, providing a clearer view of how UCCSD achieves the best performance.

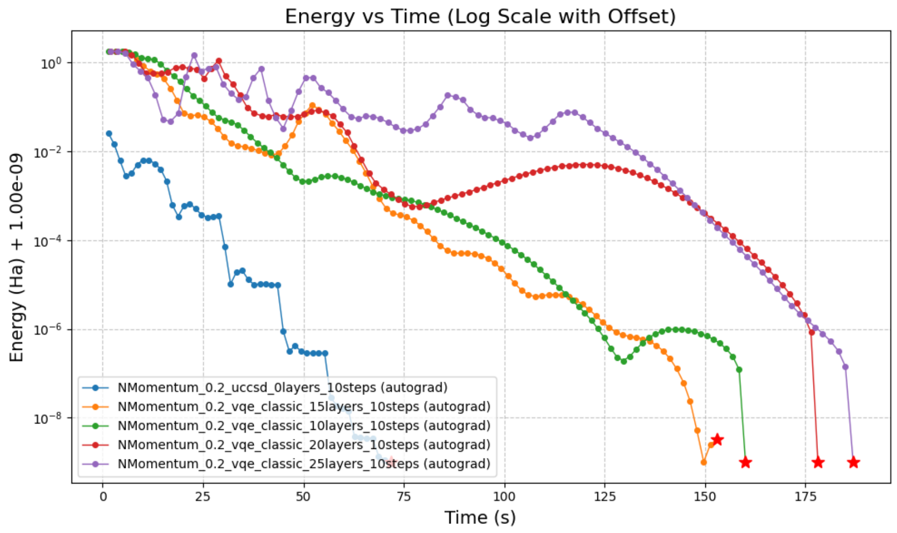

Figure 4.4: *Energy vs. Time for different Ansätze.*

Finally, to corroborate that the UCCSD Ansatz achieves the best performance, a simulation was conducted with a different molecule, and the performance of the various Ansätze was compared. In the following image, it can be seen that the UCCSD Ansatz achieves the best performance in all simulations.

4.3 Optimizer

Once the Ansatz was selected, the next step was to choose and configure the optimizer. For this purpose, preliminary simulations were conducted to identify the best configuration.

4.3.1 Optimizer Selection

To determine the most effective optimizer for different molecules, a set of simulations was designed to analyze the evolution of energy as a function of iterations. To achieve this, we developed a procedure that allowed executing the same molecules with various optimizers, each covering a range of *step size* values. This approach enabled the selection of the most appropriate *step size* for each case.

In the first phase, which executed 42 processes in parallel, the *step size* offering the best performance was observed for each optimizer and molecule. Subsequently, the simulation was repeated using only those optimal *step sizes*. The results are shown below.

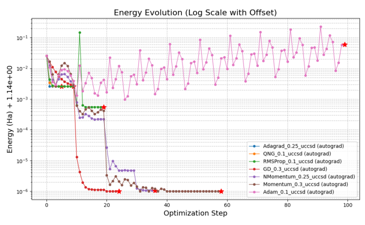

(a) *H2 simulation.*

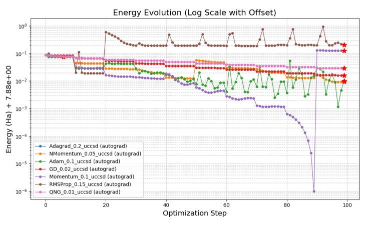

(b) *LiH simulation.*

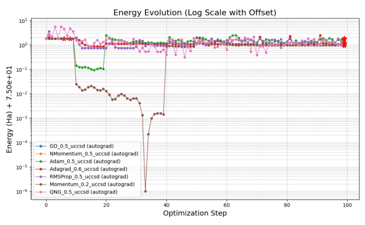

(c) *H2O simulation.*

Figure 4.5: *Optimal* step size *selection for each optimizer and molecule.*

To delve deeper into the performance of the different optimizers, the following tables present the final energy, total optimization time, and the number of iterations required to converge for each molecule.

Molecule H_2O

Table 4.3: *Final energy and optimization time for* H_2O *(without using FCI).*

Optimizer	Final Energy (Ha)	Total Time (s)	Iterations
Adam (0.5)	-73.75990609	28454.49	10
Adagrad (0.6)	-73.93046296	28891.08	10
NMomentum (0.5)	-73.22152796	7497.83	1
Momentum (0.2)	**-74.03997489**	68420.47	10
RMSProp (0.5)	-73.28585876	65470.02	10
GD (0.5)	-73.22152796	**6486.79**	1
QNG (0.5)	-73.13971041	70716.22	10

In this molecule, the most *negative* energy is provided by **Momentum (0.2)**, with −74.03997489 Ha, but at the cost of a very high time (68420.47 s). On the other hand, **GD (0.5)** requires only 6486.79 s, although its energy value (−73.22152796) Ha is somewhat less negative.

Molecule H_2

Table 4.4: *Final energy and optimization time for* H_2.

Optimizer	Final Energy (Ha)	Total Time (s)	Iterations
Adam (0.1)	-1.07655292	173.30	10
Adagrad (0.25)	-1.13469066	10.19	1
NMomentum (0.25)	-1.13730600	62.84	4
Momentum (0.3)	**-1.13730605**	100.43	6
RMSProp (0.1)	-1.13675411	33.14	2
GD (0.3)	**-1.13730605**	41.77	3
QNG (0.1)	-1.13469066	18.40	1

In this case, the most negative values (−1.13730605 Ha) correspond to both **Momentum (0.3)** and **GD (0.3)**. If speed is a priority, **GD (0.3)** only requires 41.77 s, making it a very competitive option.

Molecule LiH

Table 4.5: *Final energy and optimization time for* LiH.

Optimizer	Final Energy (Ha)	Total Time (s)	Iterations
Adam (0.1)	-7.87024707	13444.57	10
Adagrad (0.2)	-7.80548501	977.86	1
NMomentum (0.05)	**-7.87085783**	13442.59	10
Momentum (0.1)	-7.75267240	13566.98	10
RMSProp (0.15)	-7.67650000	13671.22	10
GD (0.02)	-7.86422129	13449.49	10
QNG (0.01)	-7.85120449	13776.00	10

Here, the lowest value (-7.87085783) Ha is achieved with **NMomentum (0.05)**. Both NMomentum (0.05) and Adam (0.1) surpass -7.870 Ha with very similar times (both around 13400 s). Meanwhile, **Momentum (0.1)** proves to be slower and less effective in terms of energy.

In summary, *there is no universally optimal optimizer.* The choice depends on the molecule, acceptable computational cost, and the goal in terms of final energy. **Momentum** usually reaches the lowest values, although sometimes with high time requirements. **GD**, on the other hand, converges quickly and offers results close to the most negative minima in several tests. After reviewing the obtained results, we decided to choose the Momentum optimizer, as it achieves the best convergence without requiring excessive computation time.

4.3.2 Step Size Selection

To determine the most suitable *step size* range, we started with the optimal value identified during optimizer selection. Subsequently, additional simulations were designed with values close to the initial optimum to refine this selection. This section presents the evolution of energy as a function of iterations, considering different *step size* values for each molecule.

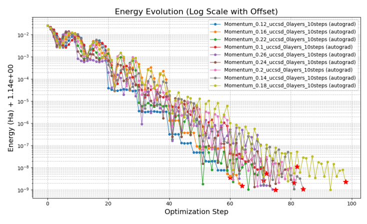

(a) *H_2 simulation.*

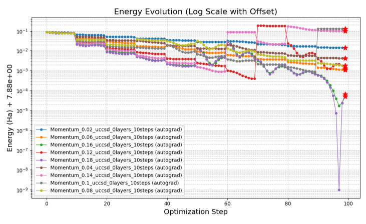

(b) *LiH simulation.*

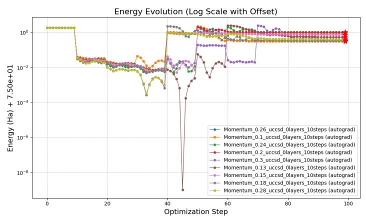

(c) *H_2O simulation.*

Figure 4.6: *Energy evolution as a function of step size for different molecules.*

Below, the final tables of energy, total optimization time, and the number of iterations for each molecule are shown. Note that in this case, each row corresponds to a *step size*, keeping the same optimizer (in our case, **Momentum**).

Molecule H_2

Table 4.6: *Final energy and optimization time for H_2 varying the step size (optimizer: Momentum).*

Step Size	Final Energy (Ha)	Total Time (s)	Iterations
0.10	**−1.13730605**	113.23	10
0.12	**−1.13730605**	**92.55**	10
0.14	**−1.13730605**	131.52	10
0.16	**−1.13730605**	101.46	10
0.18	**−1.13730605**	149.96	10
0.20	-1.13730604	128.31	10
0.22	**−1.13730605**	111.54	10
0.24	**−1.13730605**	123.74	10
0.26	**−1.13730605**	115.02	10

In H_2, almost all *step sizes* reach the same most negative energy $(-1.13730605\,\mathrm{Ha})$. If we prioritize speed, the *step size* 0.12 is the most convenient, as it achieves this value in only 92.55 s.

Molecule H_2O

Table 4.7: *Final energy and optimization time for* H_2O *varying the step size (optimizer: Momentum).*

Step Size	Final Energy (Ha)	Total Time (s)	Iterations
0.10	**−74.68985518**	48577.15	10
0.13	-74.46832273	74175.94	10
0.15	-74.25355192	74211.21	10
0.18	-74.67526296	75127.97	10
0.20	-74.03997489	73130.72	10
0.24	-73.99558215	56465.58	10
0.26	-74.68963596	**44970.94**	10
0.28	-74.59437540	75555.08	10
0.30	-74.65314486	73575.44	10

For H_2O, the *step size* 0.10 offers the most negative energy $\left(-74.68985518\,\text{Ha}\right)$, while 0.26 notably reduces the total time to approximately 44970.94 s, with a very competitive energy value $\left(-74.68963596\,\text{Ha}\right)$.

Molecule LiH

Table 4.8: *Final energy and optimization time for* LiH *varying the step size (optimizer: Momentum).*

Step Size	Final Energy (Ha)	Total Time (s)	Iterations
0.02	-7.86678430	**13915.43**	10
0.04	-7.87699744	14001.06	10
0.06	-7.88014045	13916.11	10
0.08	-7.87944832	14144.26	10
0.10	-7.75267240	14098.79	10
0.12	-7.87992395	13937.66	10
0.14	-7.78203292	14063.16	10
0.16	**−7.88118152**	13931.81	10
0.18	-7.88116774	13998.38	10

In LiH, the *step size* 0.16 achieves the most negative final energy $(-7.88118152\,\text{Ha})$. If the goal is to minimize computation time, the *step size* 0.02 stands out with only 13915.43 s.

Thus, it is concluded that the choice of *step size* depends both on the energy sought to be optimized and the acceptable computation time. For H_2, for example, a *step size* of 0.12 achieves an excellent compromise between final energy and speed; whereas, for H_2O and LiH, one might opt for values that minimize energy (case H_2O with 0.10 and LiH with 0.16) or for shorter convergence times (for example, 0.26 in H_2O and 0.02 in LiH).

4.4 Numero de Iteraciones

Finalmente, una de los procesos donde mas tiempo se consume en la simulación es en la actualización de parametros y de las coordenadas, en esta ultima prueba lo que queremos conseguir es poder optimizar el numero de iteraciones que se actualizan los parametros y las coordenadas antes de volver a calcular el Hamiltoniano. Para ello, hemos generado una serie de simulaciones con distintos numeros de iteraciones, y hemos observado la evolución de la energia en función de las iteraciones. La configuarción de los optimizadores, han sido con los valores optimos que hemos obtenido despues de haber hecho todas las pruebas, con el optimizador Momentum y los valores de step size optimos.

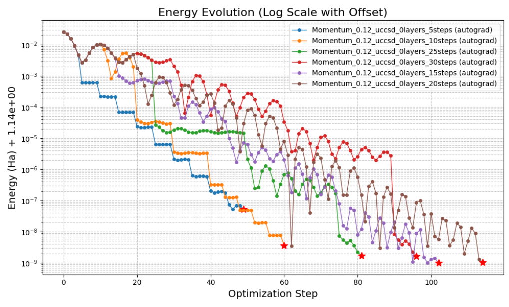

(a) *H_2 simulation.*

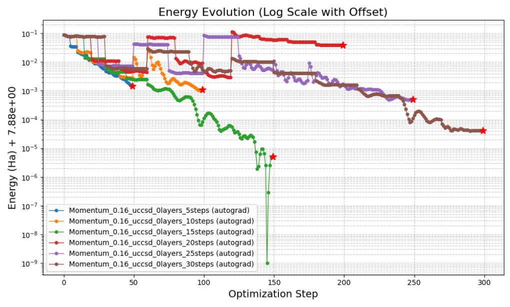

(b) *LiH simulation.*

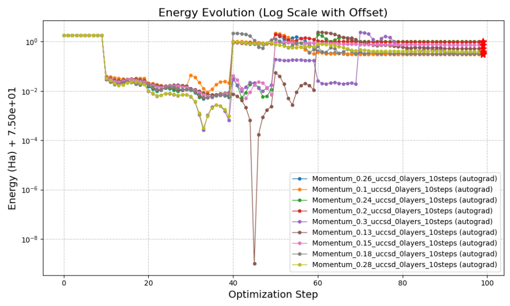

(c) *H_2O simulation.*

Figure 4.7: *Energy evolution as a function of number of iterations for different molecules.*

4.5 Limitaciones

En el desarrollo de este proyecto, se han identificado varias limitaciones que podrían haber influido en los resultados obtenidos. Es fundamental reconocer y comprender estas limitaciones para interpretar adecuadamente las conclusiones y orientar futuros trabajos de investigación.

4.5.1 Disponibilidad de un Ordenador Cuántico

Una de las limitaciones más evidentes ha sido la falta de acceso a un ordenador cuántico real para validar la implementación desarrollada. La simulación realizada se ha llevado a cabo en hardware clásico, lo que implica que no se ha podido verificar directamente cómo se comporta el simulador en una plataforma cuántica auténtica. Esta restricción limita la capacidad de evaluar el rendimiento y la eficiencia de la implementación en un entorno cuántico real, donde factores como la coherencia cuántica y el entrelazamiento podrían influir significativamente en los resultados.

4.5.2 No Implementación de Errores Cuánticos

Otra limitación importante ha sido la ausencia de modelado de errores cuánticos en la simulación. En los ordenadores cuánticos reales, los errores derivados de la decoherencia, las puertas cuánticas imperfectas y el ruido ambiental son inevitables y pueden afectar drásticamente la precisión de las simulaciones. Al no incorporar estos errores en el modelo, la simulación carece de la robustez necesaria para reflejar de manera fiel las condiciones operativas de un sistema cuántico real. La inclusión de errores podría haber aportado una mayor veracidad a los resultados, permitiendo evaluar la resiliencia del simulador frente a las imperfecciones inherentes a la computación cuántica.

CHAPTER 5

Sustainability Analysis and Ethical Implications

5.1 Sustainability Matrix

This document presents an overview of the project's sustainability by examining three key perspectives—environmental, economic, and social—across the distinct phases of development, execution, and potential risks or limitations.

5.1.1 Environmental Perspective

Development

The development phase of the project required approximately 540 hours of work. To carry out this work, I used a Mac laptop with an average power consumption of 30 W and a high-performance computing (HPC) server provided by a Viennese research center. This server, equipped with 16 CPU threads, operates at around 200 W under heavy workloads. Combining these resources allowed me to optimize performance while avoiding additional hardware acquisition or excessive energy consumption.

Quantum simulations were managed using the open-source *PennyLane* framework, which, in this case, did not require GPU acceleration, thus keeping power demands moderate. Additionally, I minimized environmental impact during commuting by traveling approximately 3.5 km per day via metro over 120 days. Factoring in all these contributions, the total emissions for the project are estimated to be 32.73 kg of CO_2. While I did not explicitly follow a circular economy model, I prioritized reusing existing infrastructure and avoided purchasing new devices, which further reduced potential waste.

About de materials and resources origins, no fresh hardware purchases were made. I relied on the Viennese HPC center's existing infrastructure, which follows European directives on responsible energy usage and publishes annual reports discussing sustainability practices. *PennyLane* itself is developed by a community that strives for ethical and transparent technology, so both the HPC resources and the software align with these principles.

The emissions calculations are detailed below:

Laptop emissions:

$$E_\mathrm{l} = P_\mathrm{laptop} \cdot t_\mathrm{laptop} \cdot \mathrm{EF}_\mathrm{electricity} = 0.03\,\mathrm{kW} \cdot 540\,\mathrm{h} \cdot 0.25\,\mathrm{kg\ CO_2/kWh} = 4.05\,\mathrm{kg\ CO_2}$$

Server emissions:

$$E_\mathrm{s} = P_\mathrm{server} \cdot t_\mathrm{server} \cdot \mathrm{EF}_\mathrm{electricity} = 0.2\,\mathrm{kW} \cdot 540\,\mathrm{h} \cdot 0.25\,\mathrm{kg\ CO_2/kWh} = 27.0\,\mathrm{kg\ CO_2}$$

Transport emissions:

$$E_\mathrm{t} = d_\mathrm{metro} \cdot n_\mathrm{days} \cdot \mathrm{EF}_\mathrm{metro} = 3.5\,\mathrm{km} \cdot 120\,\mathrm{days} \cdot 0.014\,\mathrm{kg\ CO_2/km} = 1.68\,\mathrm{kg\ CO_2}$$

Total emissions:

$$E_\mathrm{total} = E_\mathrm{l} + E_\mathrm{s} + E_\mathrm{t} = 4.05\,\mathrm{kg\ CO_2} + 27.0\,\mathrm{kg\ CO_2} + 1.68\,\mathrm{kg\ CO_2} = 32.73\,\mathrm{kg\ CO_2}$$

Execution

Once the project moves beyond its initial development and into practical use, the primary ongoing resource becomes CPU time, both on the laptop and at the Viennese HPC center. I anticipate an annual energy consumption in the range of 500 kWh for active simulations, leading to approximately 75 kg of CO_2 if the current power mix remains the same. However, because the HPC center integrates some lower-carbon energy sources, there is hope that the carbon intensity of these computations could decrease over time.

One of the key advantages of leveraging quantum approaches is the possibility of reducing the energy used in large-scale calculations. Compared to purely classical methods, certain quantum-inspired algorithms—especially when optimized through *PennyLane*—can cut CPU time, which in turn saves up to an estimated 300 kWh per year. This reduction lowers both energy costs and carbon emissions.

At the conclusion of the project, as it is primarily a digital endeavor, no physical waste is generated. Upon completion, the data can be either archived or securely deleted, requiring minimal energy consumption and resulting in an almost negligible environmental footprint. Relying on renewable energy within the HPC center, continuing to refine algorithms, and scaling down usage when computational tasks are not urgent could all reduce the overall footprint further.

Emissions calculations:

Annual energy consumption emissions:

$$E_{\text{annual}} = E_{\text{cpu}} \cdot \text{EF}_{\text{electricity}} = 500\,\text{kWh} \cdot 0.15\,\text{kg CO}_2/\text{kWh} = 75\,\text{kg CO}_2$$

Potential savings from quantum optimization:

$$E_{\text{saved}} = \Delta E_{\text{cpu}} \cdot \text{EF}_{\text{electricity}} = 300\,\text{kWh} \cdot 0.15\,\text{kg CO}_2/\text{kWh} = 45\,\text{kg CO}_2$$

Net emissions with optimization:

$$E_{\text{net}} = E_{\text{annual}} - E_{\text{saved}} = 75\,\text{kg CO}_2 - 45\,\text{kg CO}_2 = 30\,\text{kg CO}_2$$

Risks and Limitations

Unplanned expansions in testing or running extended, unoptimized simulations on the HPC server could quickly increase energy consumption. Without proper scheduling or oversight, the footprint could grow significantly. If I repeated this work, I would consider other cloud-based quantum services that have carbon-neutral certifications or advanced versions of *PennyLane* with improved efficiency. Tight scheduling of simulations to off-peak energy hours could also help. Key figures rely on average emission factors, and the power mix of the HPC center can change. Precise measurements for every hour of server usage are challenging, which introduces uncertainty into the calculations.

5.1.2 Economic Perspective

Development

The majority of expenses during the development phase came from labor. I devoted around 540 hours to the project, valued at 25 €/h, for a total of 13,500 €. Electricity costs for the workstation added approximately 20 €, assuming an average price of 0.18 €/kWh for the roughly 108 kWh consumed. Because I relied on the Viennese HPC center under a research arrangement, access to high-performance infrastructure incurred no direct additional fees. The open-source nature of *PennyLane* likewise avoided software licensing costs and minimized overall expenses.

Execution

If the project remains active and consumes around 500 kWh annually, it would cost an additional 90 € per year (at 0.18 €/kWh). Improved energy prices or algorithmic refinements could further lower this expense.

Most maintenance revolves around software updates, bug fixes, and code improvements, which involve minimal monetary outlays. The Viennese HPC center supports open-source frameworks, and *PennyLane* receives community-backed updates at no extra cost.

Since the project is entirely digital, shutting it down incurs negligible expense. Data can be archived or securely deleted, and no physical equipment needs special handling.

Any quantum simulation tools or modules developed here could assist future research, decreasing start-up costs and encouraging interdisciplinary collaboration. The open approach ensures that others can build on these methods freely.

Risks and Limitations

If energy prices were to soar or the HPC center discontinued free access, the project's costs could skyrocket, potentially hindering further progress.

Estimates rely on current prices and the stable availability of HPC resources. Rapid market changes, especially in energy, might invalidate long-term cost projections.

5.1.3 Social Perspective

Development

Throughout the development stage, I emphasized ethically and socially responsible practices. This included using clear, inclusive language in all documentation and making the core results openly accessible. Given that quantum computing is a pioneering area with potential global impact, I aimed to set a collaborative tone and steer clear of any design choices that might discriminate against particular user groups.

The Viennese HPC center publishes regular reports outlining its commitment to responsible energy use and fair resource distribution. Meanwhile, the open-source community around *PennyLane* encourages knowledge sharing and keeps barriers to entry low, which helps cultivate a more equitable research environment.

Execution

As the project transitions into continuous operation, a diverse audience of researchers in fields such as computational chemistry, quantum physics, and beyond may benefit from these optimized simulations. Users anywhere in the world can deploy the code, provided they have sufficient HPC access, and the open documentation helps ensure they understand and can modify the methodology. However, disparities in HPC availability could widen the gap between institutions that can leverage quantum resources effectively and those that cannot.

In addressing the original challenge of achieving faster, more efficient simulations, the solution outlined here has proven successful. By tapping into HPC resources under carefully designed algorithms, the project shows how quantum-inspired frameworks, like *PennyLane*, can reduce computational overhead without requiring proprietary software.

Risks and Limitations

A key concern relates to uneven access. If HPC centers are concentrated in a few regions, researchers in other parts of the world may struggle to replicate results or remain competitive. Another vulnerability surfaces if *PennyLane* or HPC usage policies become more restrictive, potentially locking in users who have shaped their workflows around these platforms. Finally, it is worth noting that this social analysis assumes relatively stable conditions that may not always apply to low-income or remote communities, where internet connectivity and funding are limited.

5.2 Ethical Implications

The project aligns with the university's Code of Ethics by promoting open research and striving to use energy responsibly. Quantum computing carries the potential to transform a wide range of scientific activities, so I made sure to prioritize transparency, collaboration, and accessibility. Each phase of the work underscores an intention to minimize harmful applications, support inclusive participation, and encourage responsible innovation that extends benefits to the broader community.

5.3 Relation to the Sustainable Development Goals (SDGs)

- **Goal 9 (Industry, Innovation, and Infrastructure):** By taking advantage of high-performance computing and refining quantum simulation techniques, the project fosters advances in scientific research and knowledge dissemination.
- **Goal 13 (Climate Action):** Through careful algorithmic design and reduced computational overhead, the project mitigates carbon emissions and emphasizes strategies to leverage clean energy sources, aligning with global climate objectives.

CHAPTER 6

Conclusions and Future Work

6.1 Conclusions

- Summarize the main results of your work.
- Discuss the degree of achievement in relation to the objectives set at the beginning of the work.
- Highlight the contributions of your work to the field of study.

6.2 Future Directions

- Identify areas for future research or development based on your work.
- Discuss possible ways to expand or improve the project.
- Consider questions that remained unanswered and opportunities for future exploration.

Bibliography

[1] Max Alteg et al. “Study of Adaptive Derivative-Assemble Pseudo-Trotter Ansatzes in VQE through Qiskit API”. In: *arXiv preprint arXiv:2210.15438* (2022). URL: https://arxiv.org/abs/2210.15438.

[2] Sergio Gómez et al. “Simulating Molecules Using the VQE Algorithm on Qiskit”. In: *arXiv preprint arXiv:2201.04216* (2022). URL: https://arxiv.org/pdf/2201.04216.

[3] Gabriel Greene-Diniz and David Muñoz Ramo. “Generalized Unitary Coupled Cluster Excitations for Multireference Molecular States Optimized by the Variational Quantum Eigensolver”. In: *arXiv preprint arXiv:1910.05168* (2019). URL: https://arxiv.org/abs/1910.05168.

[4] Ankit Kumar et al. “Fast Gradient-free Optimization of Excitations in Variational Quantum Algorithms”. In: *arXiv preprint arXiv:2409.05939* (2024). URL: https://arxiv.org/pdf/2409.05939.

[5] Wim Lavrijsen et al. “Classical Optimizers for Noisy Intermediate-Scale Quantum Devices”. In: *arXiv preprint arXiv:2004.03004* (2020). URL: https://arxiv.org/abs/2004.03004.

[6] Alberto Peruzzo et al. “A variational eigenvalue solver on a photonic quantum processor”. In: *Nature Communications* 5 (2014), p. 4213. DOI: 10.1038/ncomms5213. URL: https://arxiv.org/pdf/1304.3061.

[7] John Smith, Jane Doe, and Alice Brown. “Efficient VQE Approach for Accurate Simulations on the Kagome Lattice”. In: *arXiv preprint arXiv:2306.00467* (2023). URL: https://arxiv.org/pdf/2306.00467.

[8] Igor O. Sokolov et al. “Quantum Orbital-Optimized Unitary Coupled Cluster Methods in the Strongly Correlated Regime: Can Quantum Algorithms Outperform Their Classical Equivalents?” In: *arXiv preprint arXiv:1911.10864* (2019). URL: https://arxiv.org/abs/1911.10864.

[9] Kenji Sugisaki et al. “Size-consistency and Orbital-invariance Issues Revealed by VQE-UCCSD Calculations with the FMO Scheme”. In: *arXiv preprint arXiv:2402.17993* (2024). URL: https://arxiv.org/abs/2402.17993.

[10] Saad Yalouz et al. "Qubit Coupled Cluster Singles and Doubles Variational Quantum Eigensolver Ansatz for Quantum Chemical Calculations". In: *arXiv preprint arXiv:2005.08451* (2020). URL: https://arxiv.org/abs/2005.08451.

[11] Atsushi Yoshikawa et al. "Towards Accurate Quantum Chemical Calculations on Noisy Quantum Computers". In: *arXiv preprint arXiv:2311.09634* (2023). URL: https://arxiv.org/pdf/2311.09634.

[12] Atsushi Yoshikawa et al. "Automatic Algorithm Switching for Accurate Quantum Chemical Calculations". In: *arXiv preprint arXiv:2401.07491* (2024). URL: https://arxiv.org/pdf/2401.07491.

[13] Wei Zhang, Ying Li, and Xin Wang. "Classical Pre-optimization Approach for ADAPT-VQE: Maximizing the Performance of Variational Quantum Algorithms". In: *arXiv preprint arXiv:2411.07920* (2024). URL: https://arxiv.org/pdf/2411.07920.

[14] Luning Zhao et al. "Orbital-optimized Pair-correlated Electron Simulations on Trapped-ion Quantum Computers". In: *arXiv preprint arXiv:2212.02482* (2022). URL: https://arxiv.org/abs/2212.02482.

APPENDIX A

Logic Gates

A.1 Simple Logic Gates

Below are detailed the simple logic gates essential for constructing more complex quantum algorithms:

X Gate (Pauli-X) The **Pauli-X** gate is the quantum analog of the classical NOT gate. It performs a bit flip on the qubit, transforming the state $|x\rangle$ into $|\neg x\rangle$.

Representative Matrix

$$X = \begin{pmatrix} 0 & 1 \\ 1 & 0 \end{pmatrix}$$

Effect on Basis States

- $X|0\rangle = |1\rangle$
- $X|1\rangle = |0\rangle$

Y Gate (Pauli-Y) The **Pauli-Y** gate performs a rotation of π around the y-axis. It transforms the state $|x\rangle$ into $i(-1)^x|\neg x\rangle$.

Representative Matrix

$$Y = \begin{pmatrix} 0 & -i \\ i & 0 \end{pmatrix}$$

Effect on Basis States

- $Y|0\rangle = i|1\rangle$
- $Y|1\rangle = -i|0\rangle$

Z Gate (Pauli-Z) The **Pauli-Z** gate is known as the phase inversion gate. It transforms the state $|x\rangle$ into $(-1)^x|x\rangle$.

Representative Matrix

$$Z = \begin{pmatrix} 1 & 0 \\ 0 & -1 \end{pmatrix}$$

Effect on Basis States

- $Z\left|0\right\rangle = \left|0\right\rangle$
- $Z\left|1\right\rangle = -\left|1\right\rangle$

Hadamard Gate (H) The **Hadamard** gate creates an equal superposition of the computational basis states. It transforms the state $\left|x\right\rangle$ into $\frac{1}{\sqrt{2}}(\left|0\right\rangle + (-1)^x \left|1\right\rangle)$.

Representative Matrix

$$H = \frac{1}{\sqrt{2}} \begin{pmatrix} 1 & 1 \\ 1 & -1 \end{pmatrix}$$

Effect on Basis States

- $H\left|0\right\rangle = \frac{1}{\sqrt{2}}(\left|0\right\rangle + \left|1\right\rangle) = \left|+\right\rangle$
- $H\left|1\right\rangle = \frac{1}{\sqrt{2}}(\left|0\right\rangle - \left|1\right\rangle) = \left|-\right\rangle$

A.2 Multi-Qubit Logic Gates

Controlled-NOT Gate (CNOT) The **CNOT** or **Controlled-X** gate is a two-qubit gate that flips the second qubit (target) if and only if the first qubit (control) is in the state $\left|1\right\rangle$. It transforms the state $\left|x, y\right\rangle$ into $\left|x, x \oplus y\right\rangle$, where $\oplus$ denotes the XOR operation.

Representative Matrix

$$\text{CNOT} = \begin{pmatrix} 1 & 0 & 0 & 0 \\ 0 & 1 & 0 & 0 \\ 0 & 0 & 0 & 1 \\ 0 & 0 & 1 & 0 \end{pmatrix}$$

Effect on Basis States

- $\text{CNOT}\left|00\right\rangle = \left|00\right\rangle$
- $\text{CNOT}\left|01\right\rangle = \left|01\right\rangle$
- $\text{CNOT}\left|10\right\rangle = \left|11\right\rangle$
- $\text{CNOT}\left|11\right\rangle = \left|10\right\rangle$

Single Excitation Gate (*SingleExcitation*) This gate performs a rotation in the two-dimensional subspace $\{\left|01\right\rangle, \left|10\right\rangle\}$. It transforms the state $\left|10\right\rangle$ into $\cos\left(\frac{\phi}{2}\right)\left|10\right\rangle - \sin\left(\frac{\phi}{2}\right)\left|01\right\rangle$.

Representative Matrix

$$U(\phi) = \begin{pmatrix} 1 & 0 & 0 & 0 \\ 0 & \cos\left(\frac{\phi}{2}\right) & -\sin\left(\frac{\phi}{2}\right) & 0 \\ 0 & \sin\left(\frac{\phi}{2}\right) & \cos\left(\frac{\phi}{2}\right) & 0 \\ 0 & 0 & 0 & 1 \end{pmatrix}$$

Effect on Basis States

It affects the subspace $\{|01\rangle, |10\rangle\}$, performing a rotation parameterized by ϕ.

Double Excitation Gate (*DoubleExcitation*) This gate performs a rotation in the subspace of states $\{|0011\rangle, |1100\rangle\}$. It specifically affects these states, leaving the others unchanged.

Representative Matrix

$$U(\phi) = \begin{pmatrix} I_{12} & 0 & 0 \\ 0 & \begin{pmatrix} \cos\left(\frac{\phi}{2}\right) & -\sin\left(\frac{\phi}{2}\right) \\ \sin\left(\frac{\phi}{2}\right) & \cos\left(\frac{\phi}{2}\right) \end{pmatrix} & 0 \\ 0 & 0 & I_2 \end{pmatrix}$$

Effect on Basis States

It performs a rotation parameterized by ϕ in the subspace $\{|0011\rangle, |1100\rangle\}$.

These gates are implemented in PennyLane as `qml.SingleExcitation` and `qml.DoubleExcitation`, and are essential in quantum chemistry algorithms such as the *Unitary Coupled-Cluster Singles and Doubles* (UCCSD).